



THE INSTITUTE OF PAPER CHEMISTRY, APPLETON, WISCONSIN

SLIDE MATERIAL

for the

~~PPC~~ - PAPER PROPERTIES AND USES

PROJECT ADVISORY COMMITTEE

MEETING

March 22-23, 1984
The Institute of Paper Chemistry
Continuing Education Center
Appleton, Wisconsin

SLIDE MATERIAL
PROJECT ADVISORY COMMITTEE
PAPER PROPERTIES AND USES

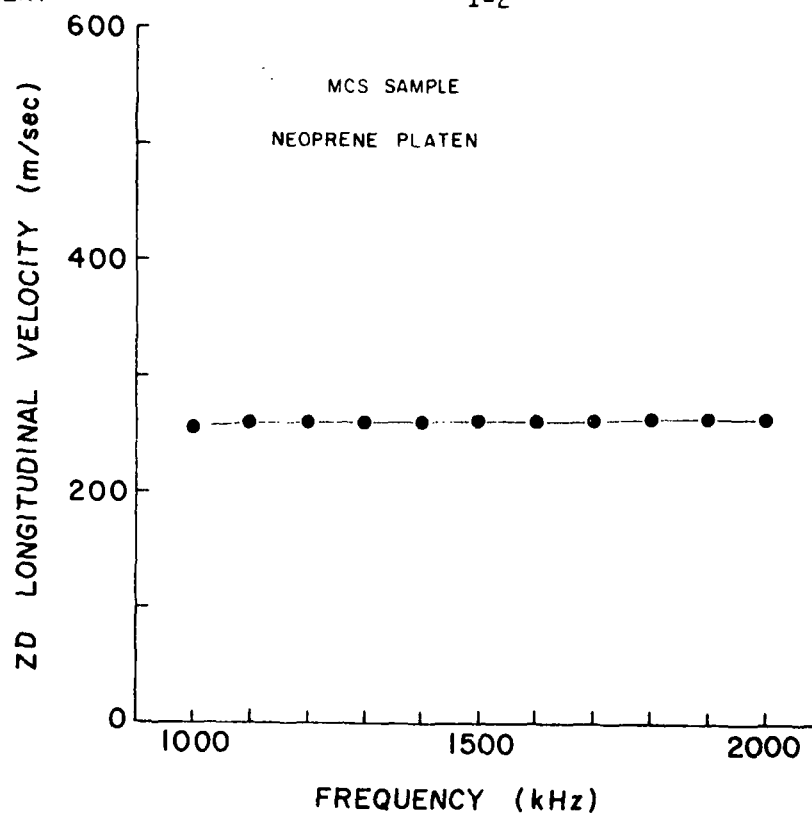
Table of Contents

	<u>Section</u>
Project 3467 -- Process, Properties, Product Relationships	1
Project 3332 -- On-line Measurement of Paper Mechanical Properties	2
Project 3500 -- Shear Deformation and Failure	3
Project 3527 -- Measurement of Fiber Properties and Fiber-to-Fiber Bonding	4
Project 3526 -- Fundamentals of Internal Strength Enhancement	5
Project 3396 -- Mechanics of Fluting	6
Project 3469 -- Compressive Strength	7
Project 3272 -- Analysis of Board Structures	8

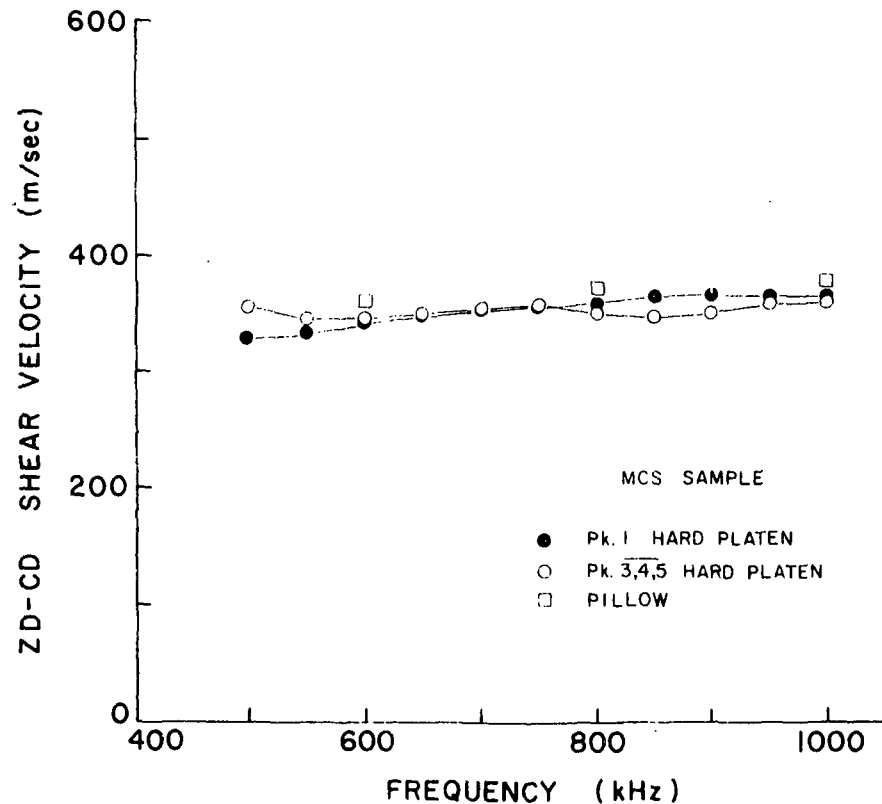
SECTION 1

PROJECT 3467

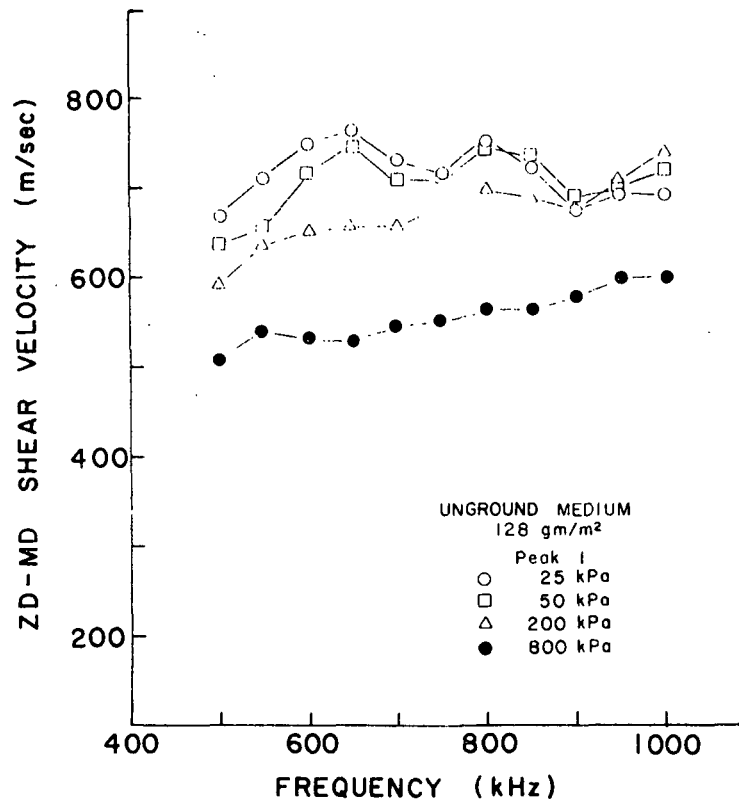
PROCESS, PROPERTIES, PRODUCT RELATIONSHIPS



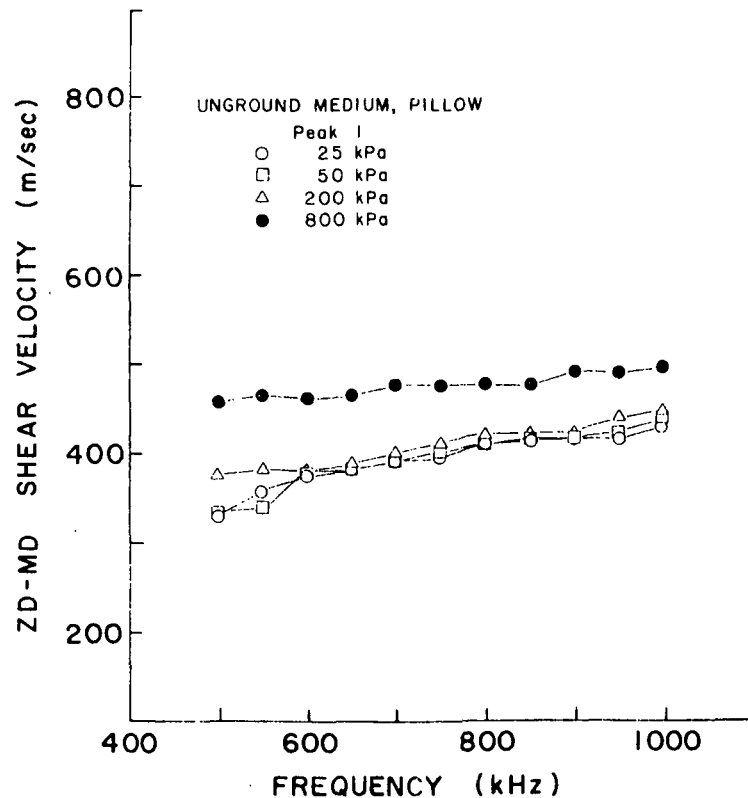
Neoprene platen, ZD longitudinal velocities vs. frequency for a machine-made bleached kraft paperboard. Hard caliper = $705 \mu\text{m}$; neoprene caliper = $692 \mu\text{m}$; $R = 0.019$.



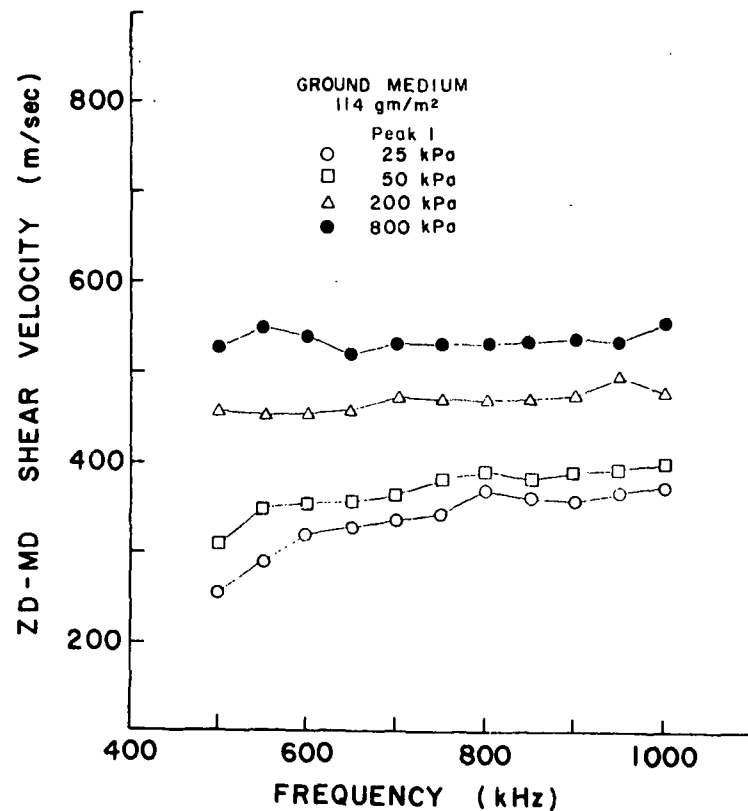
ZD-CD shear velocities vs. frequency for the MCS sample. Hard platen time of flight, pillow time of flight, and hard platen pk. 3,4,5 data are shown.



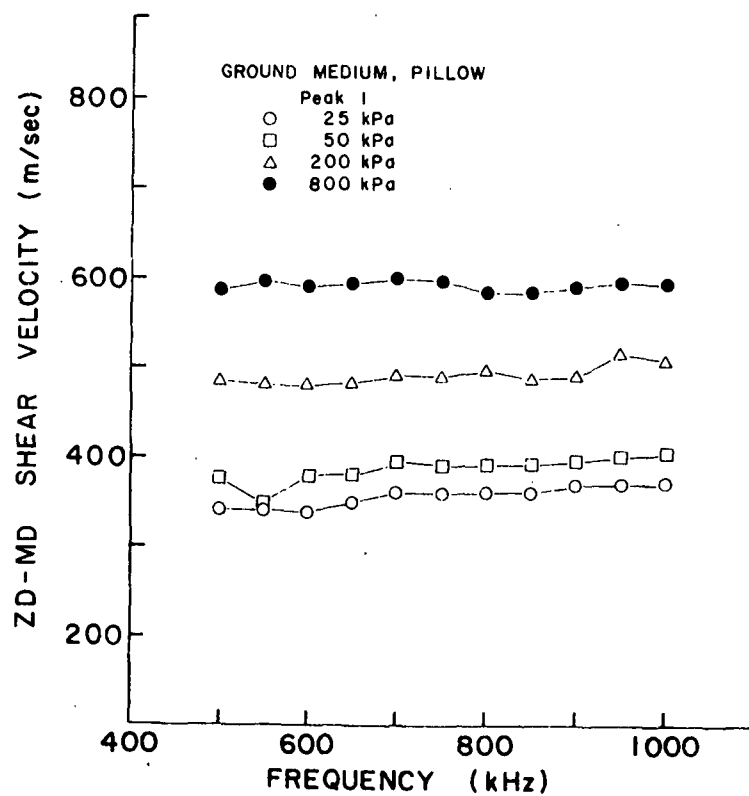
ZD-MD shear velocity vs. frequency pk. 1 time of flight, hard platen data for unground 26 lb/1000 ft² corrugating medium. Data are given for loading pressures of 25, 50, 200, and 800 kPa.



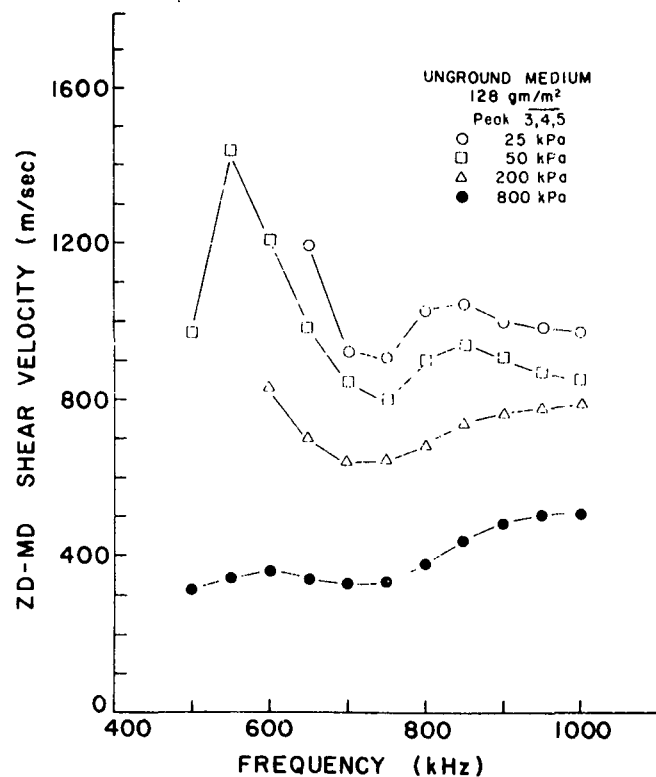
ZD-MD pillow, pk. 1 data for the unground medium sample of figure above.



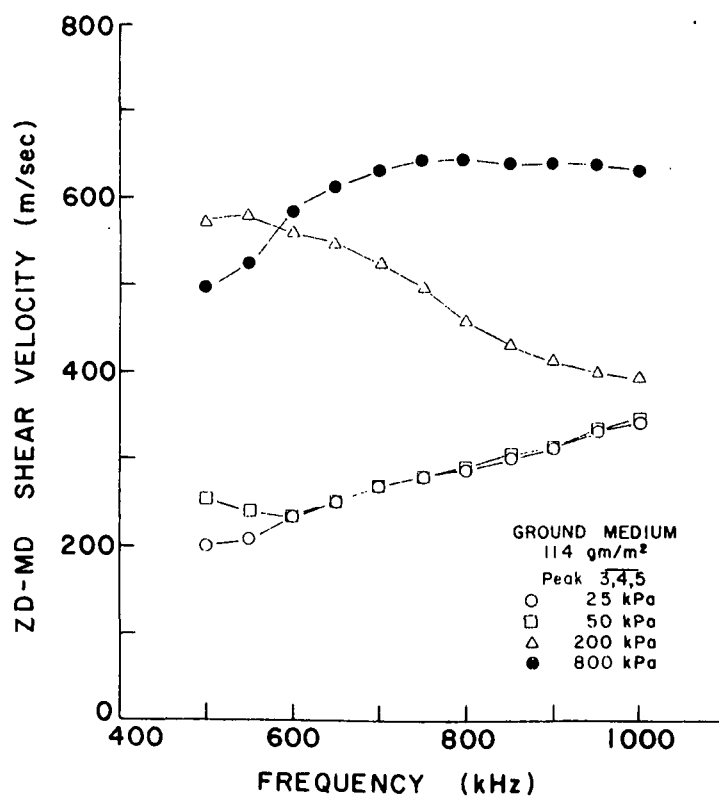
The same plots as figure top of page 1-3 for a medium with a small amount of surface grinding on each side.



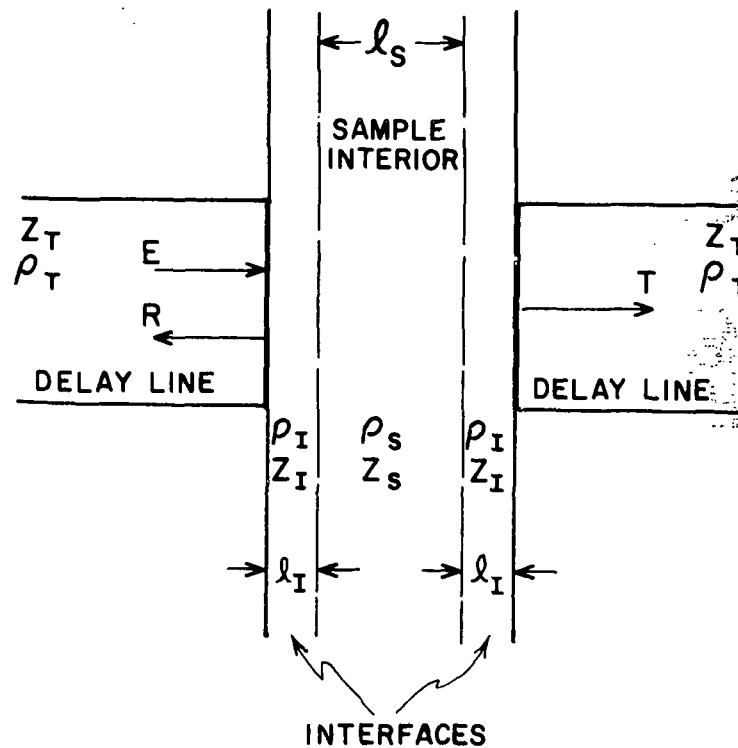
ZD-MD pillow, pk. 1 data for the ground medium.



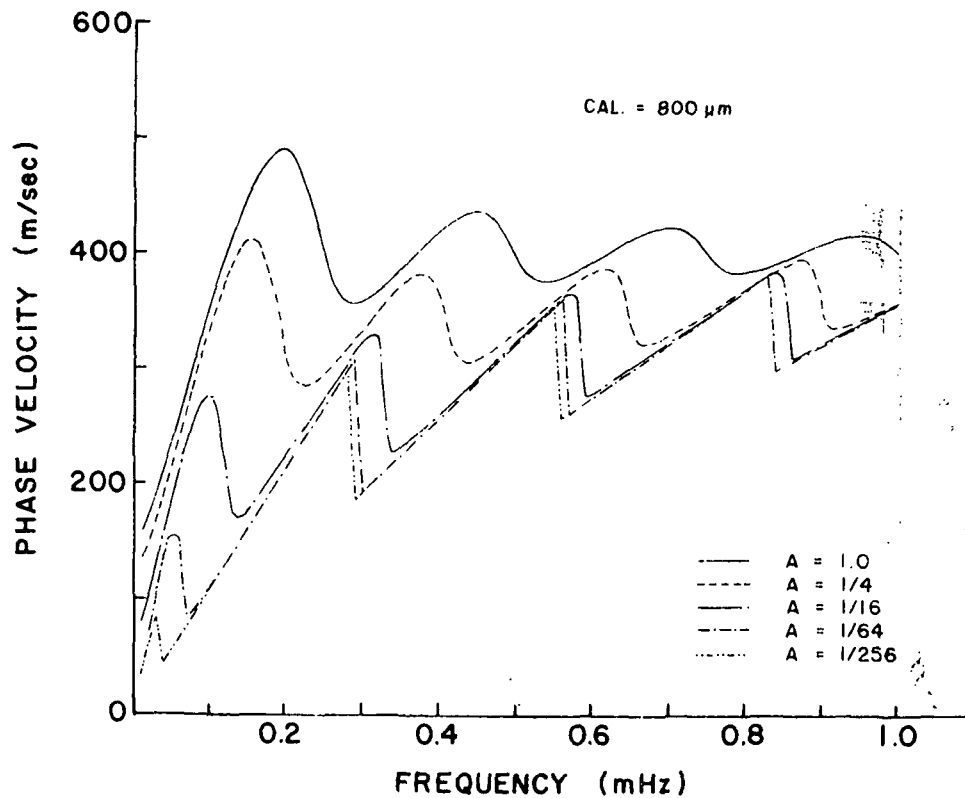
Hard platen velocity vs. frequency curves for the unground medium calculated by averaging the apparent time of flight for peaks 3, 4, and 5.



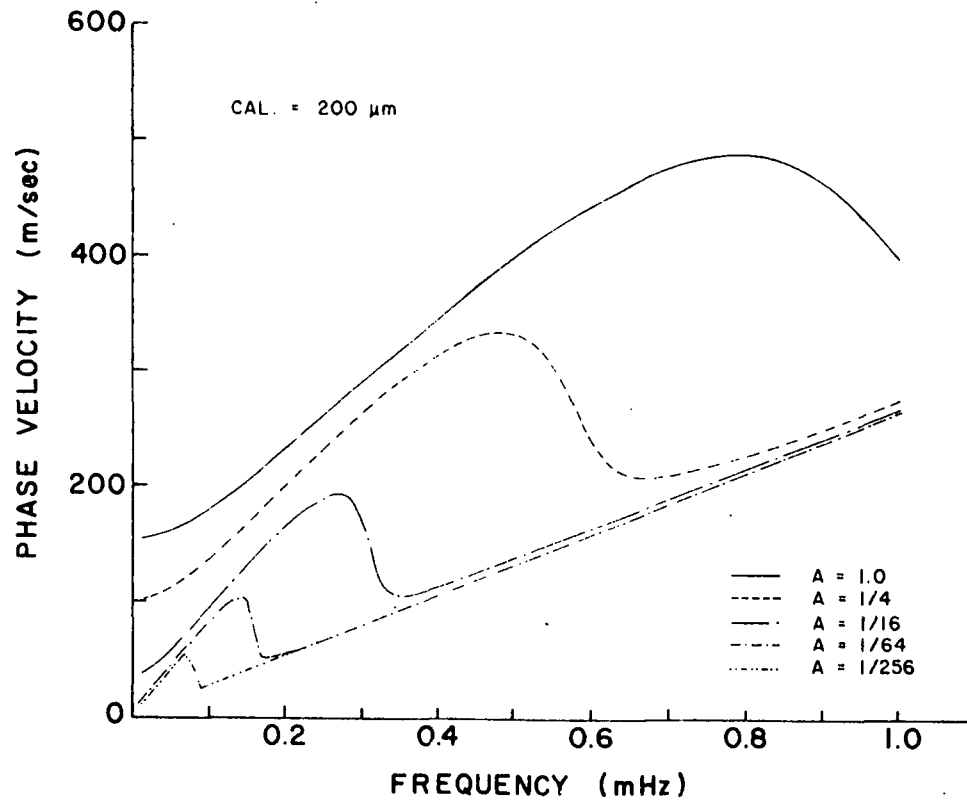
The same plots as figure above for the ground sample.



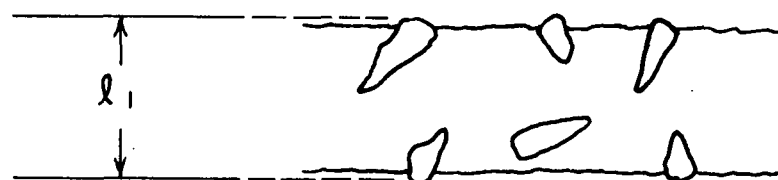
A schematic of a sample with rough interfaces, placed between delay lines in a phase velocity test.



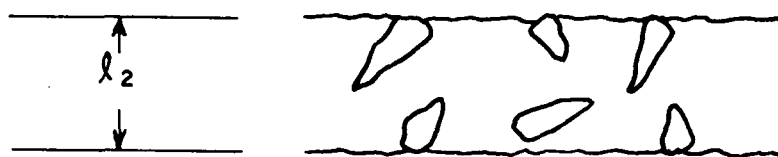
Theoretical plots of the apparent phase velocity vs. frequency for a $800 \mu m$ sample with an apparent density of 600 kg/m^3 , an interior phase velocity of 400 m/sec , an interface thickness of $40 \mu m$, and a loss tangent of zero. The interface density is A multiplied by 600 kg/m^3 , and its phase velocity is also 400 m/sec .



The same plots as previous figure but for a 200 μm thick sample.



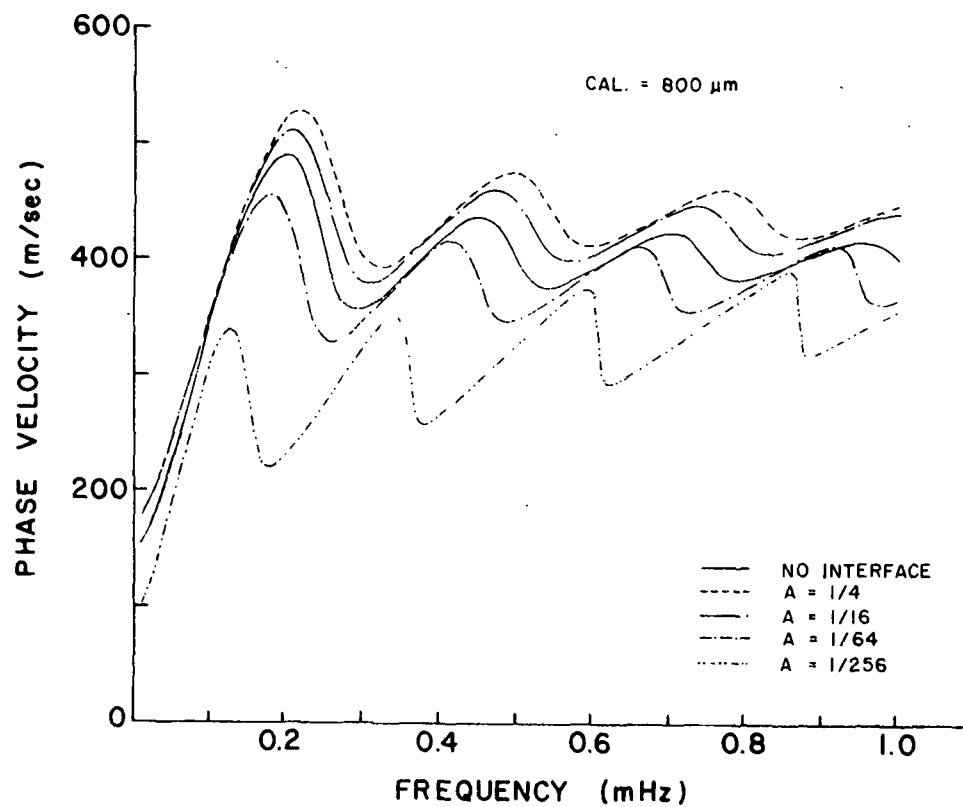
LOW PRESSURE



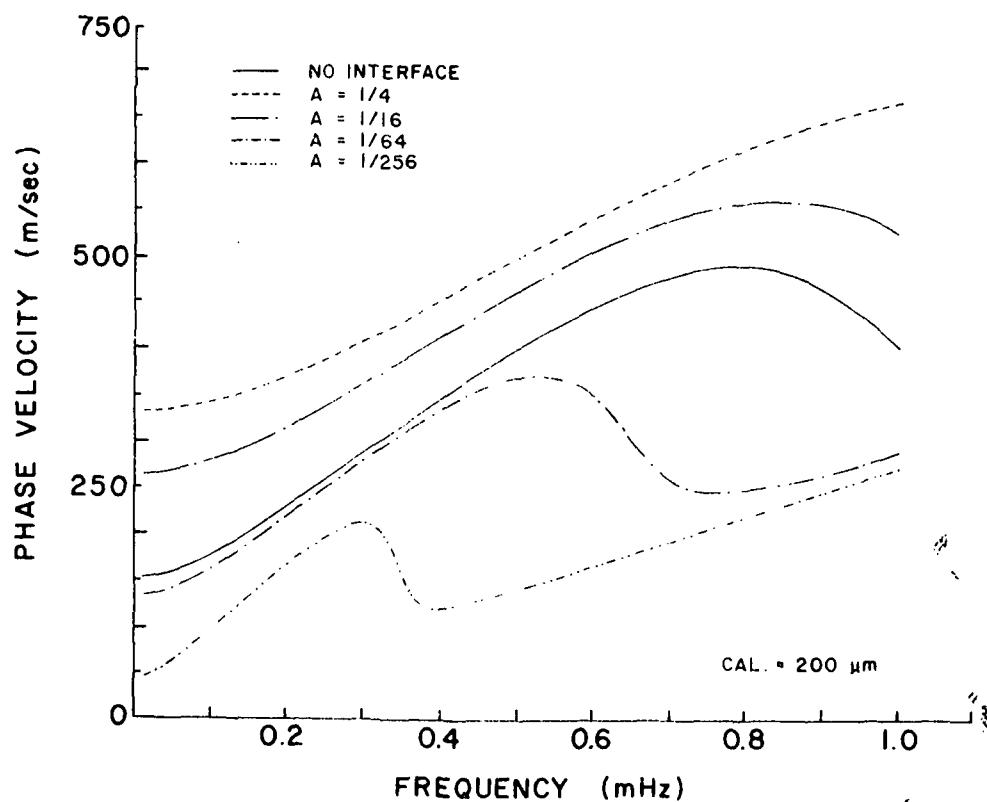
HIGH PRESSURE

$$l_1 > l_2$$

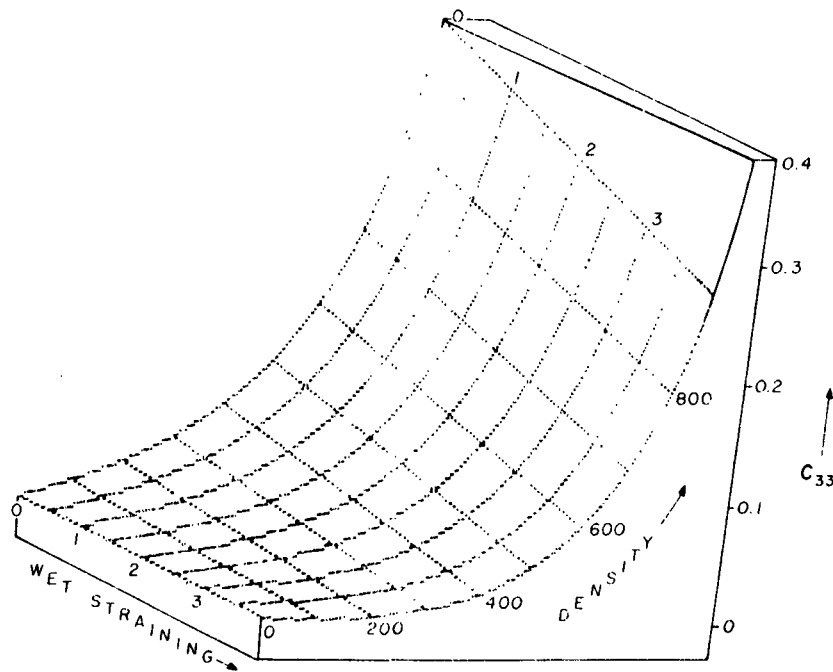
Idealized model of surface characteristics of a rough paper sample.



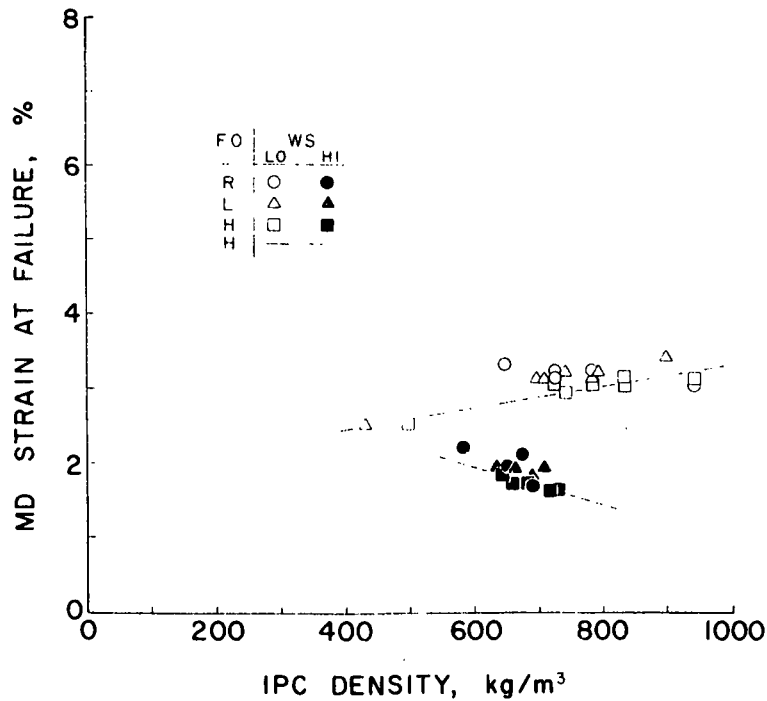
Theoretical plots of the apparent phase velocity vs. frequency for a 800- μm sample whose interior phase velocity is 400 m/sec and surface phase velocity is 2000 m/sec. $\rho = 600 \text{ kg/m}^2$, $\ell_I = 40 \text{ } \mu\text{m}$, $\tan \delta = 0$, $\ell_I = A\rho$, and $2\ell_I + \ell_S = 800 \text{ } \mu\text{m}$.



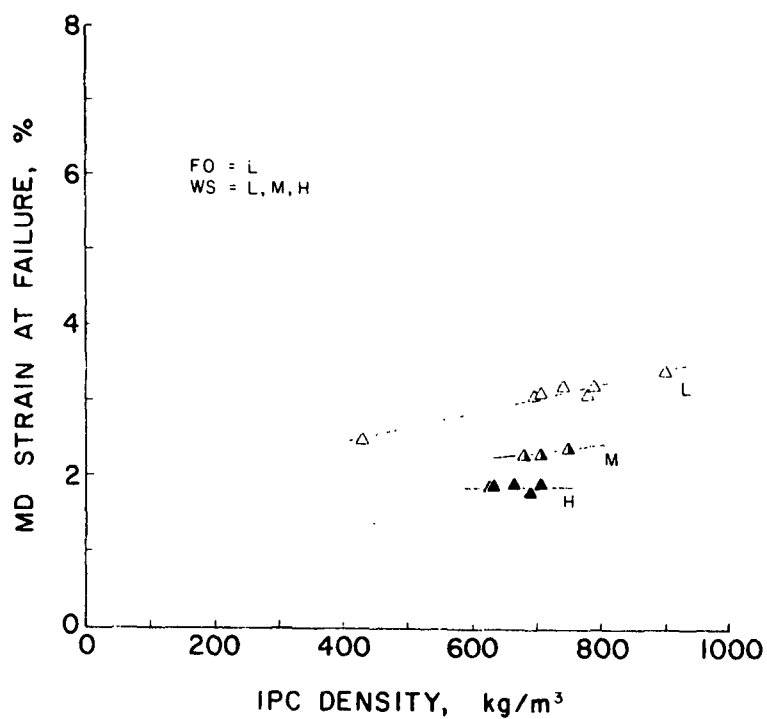
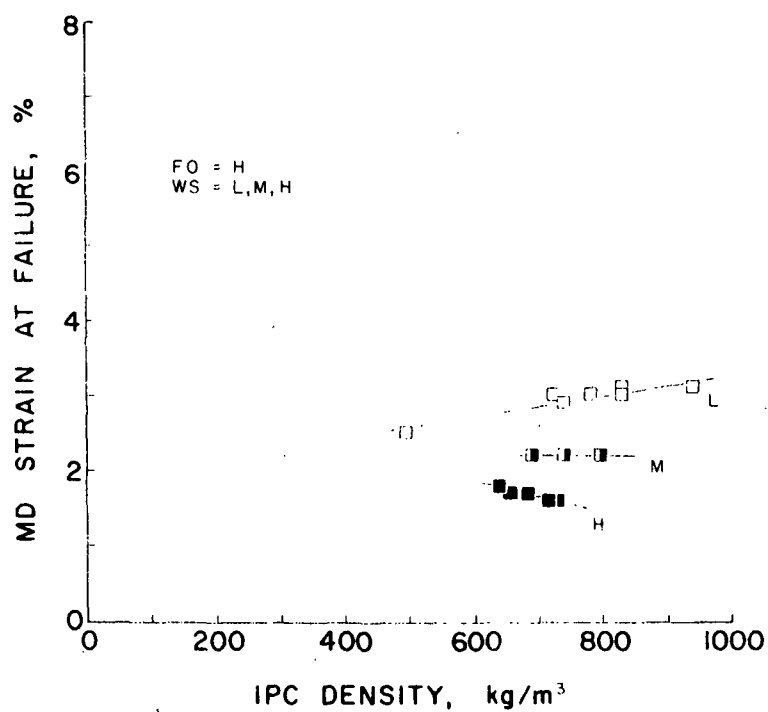
The same plots as figure above but with caliper of 200 μm .

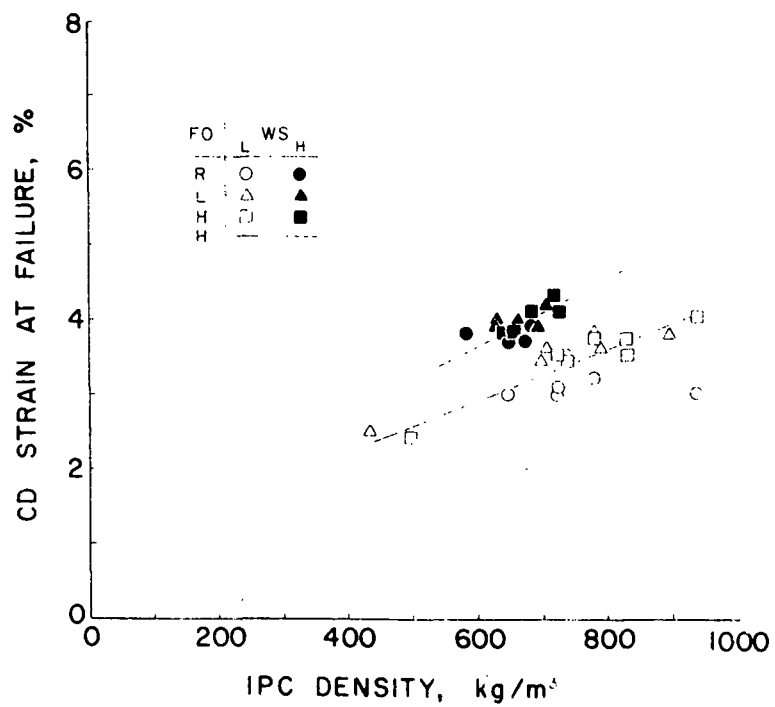
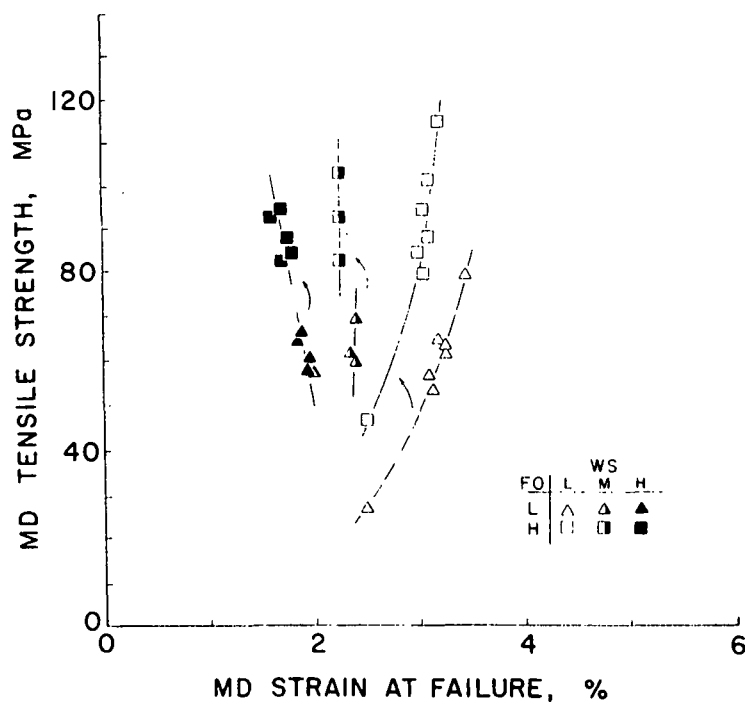


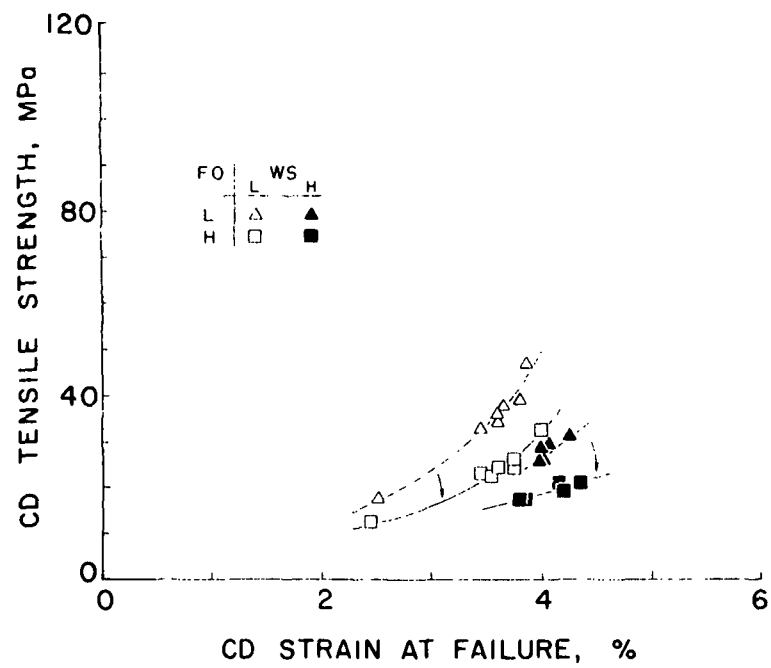
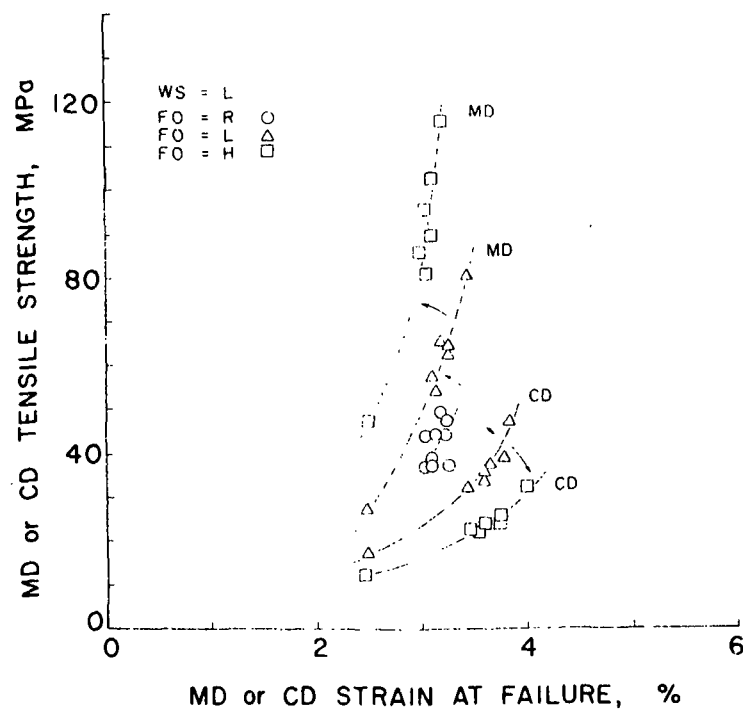
The effects of wet straining and density (wet pressing) on the out-of-plane elastic stiffness, C_{33} .

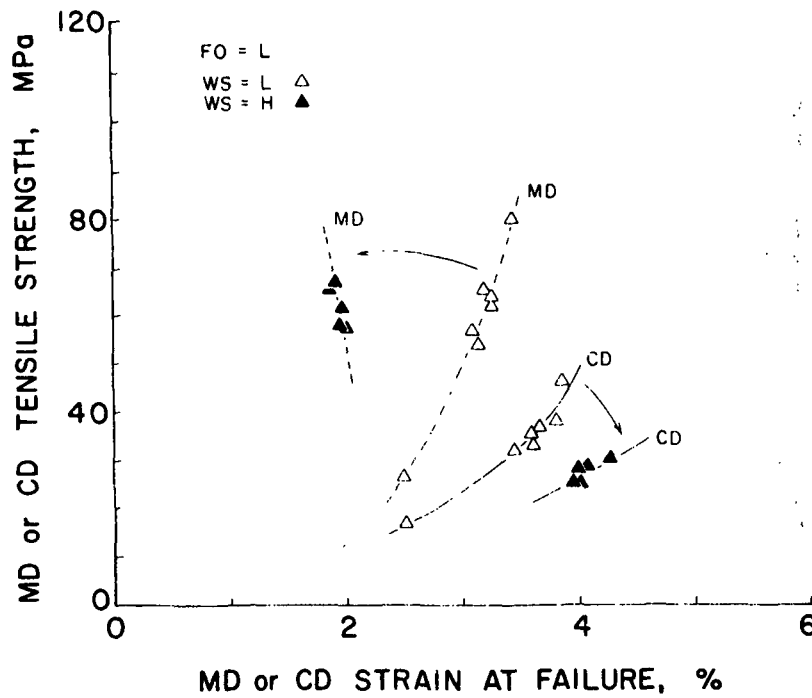


MD strain at failure vs. IPC density.

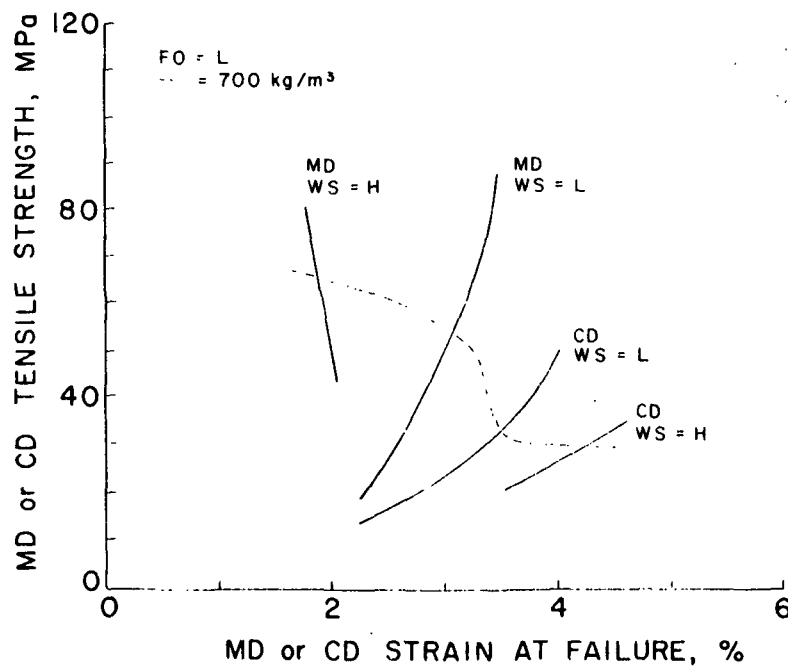
MD strain at failure vs. IPC density.MD strain at failure vs. IPC density.

CD Strain at failure vs. IPC density.MD tensile strength vs. MD strain at failure.

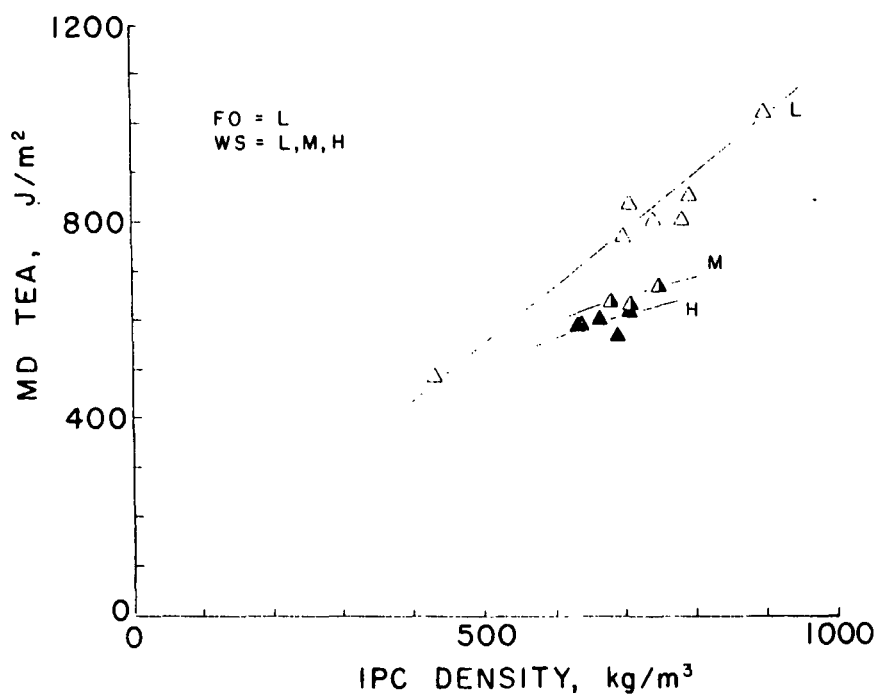
CD tensile strength vs. CD strain at failure.MD or CD tensile strength vs. MD or CD strain at failure.

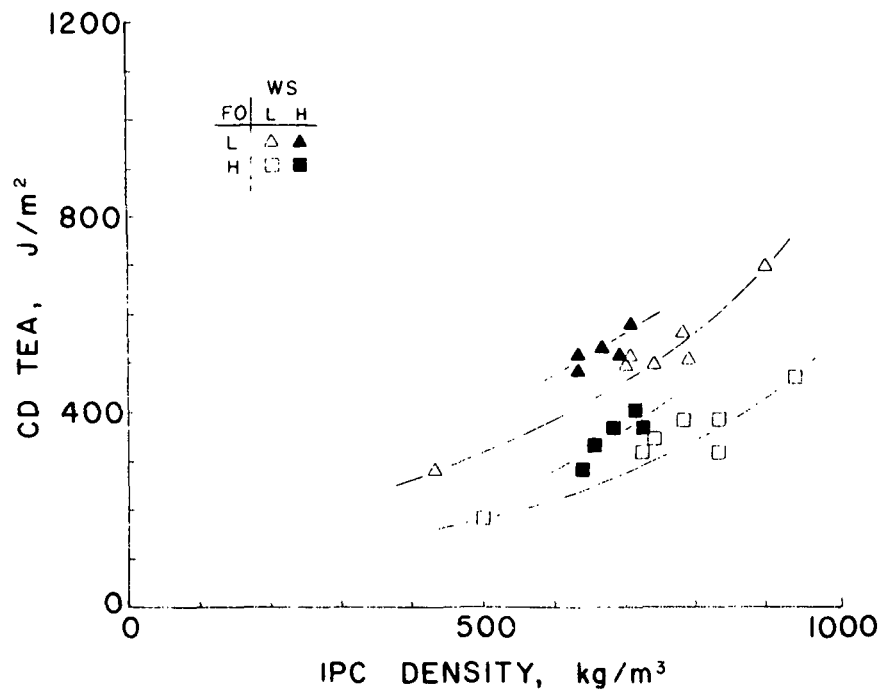


MD or CD tensile strength vs. MD or CD strain at failure.



MD or CD tensile strength vs. MD or CD strain at failure with constant density line of 700 kg/m³.



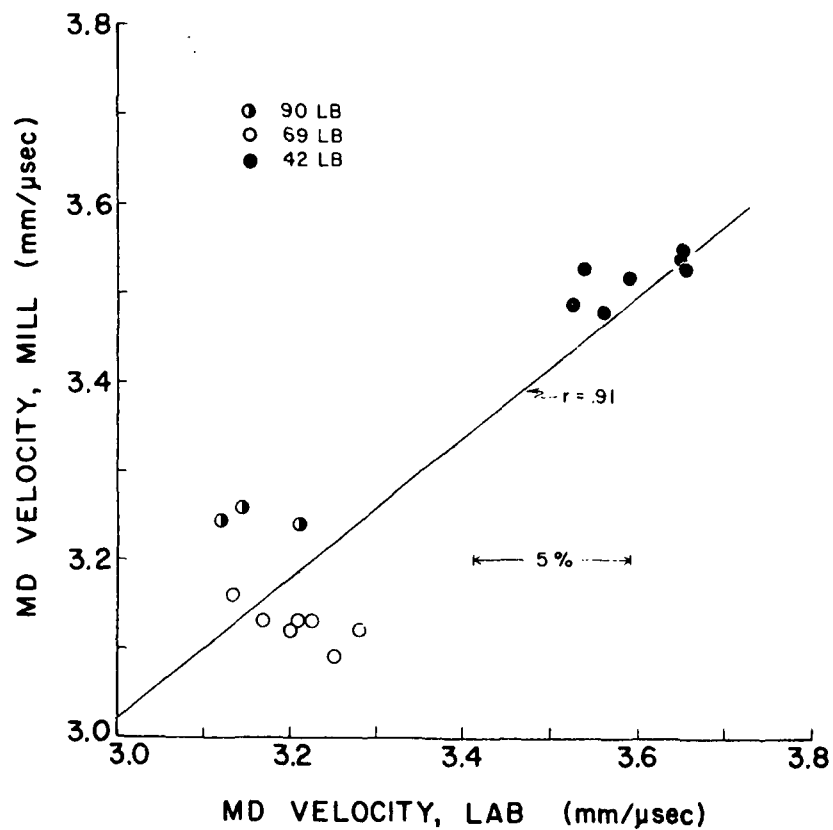


CD TEA vs. IPC density.

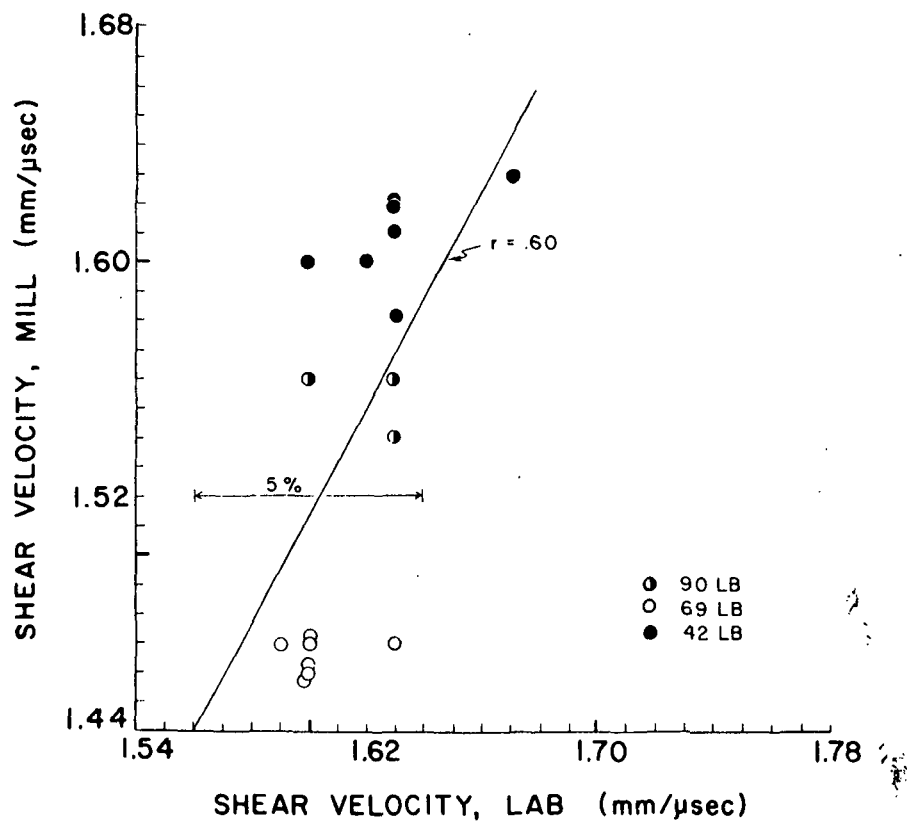
SECTION 2

PROJECT 3332

ON-LINE MEASUREMENT OF PAPER MECHANICAL PROPERTIES



MD mill velocity vs. the laboratory MD velocity.



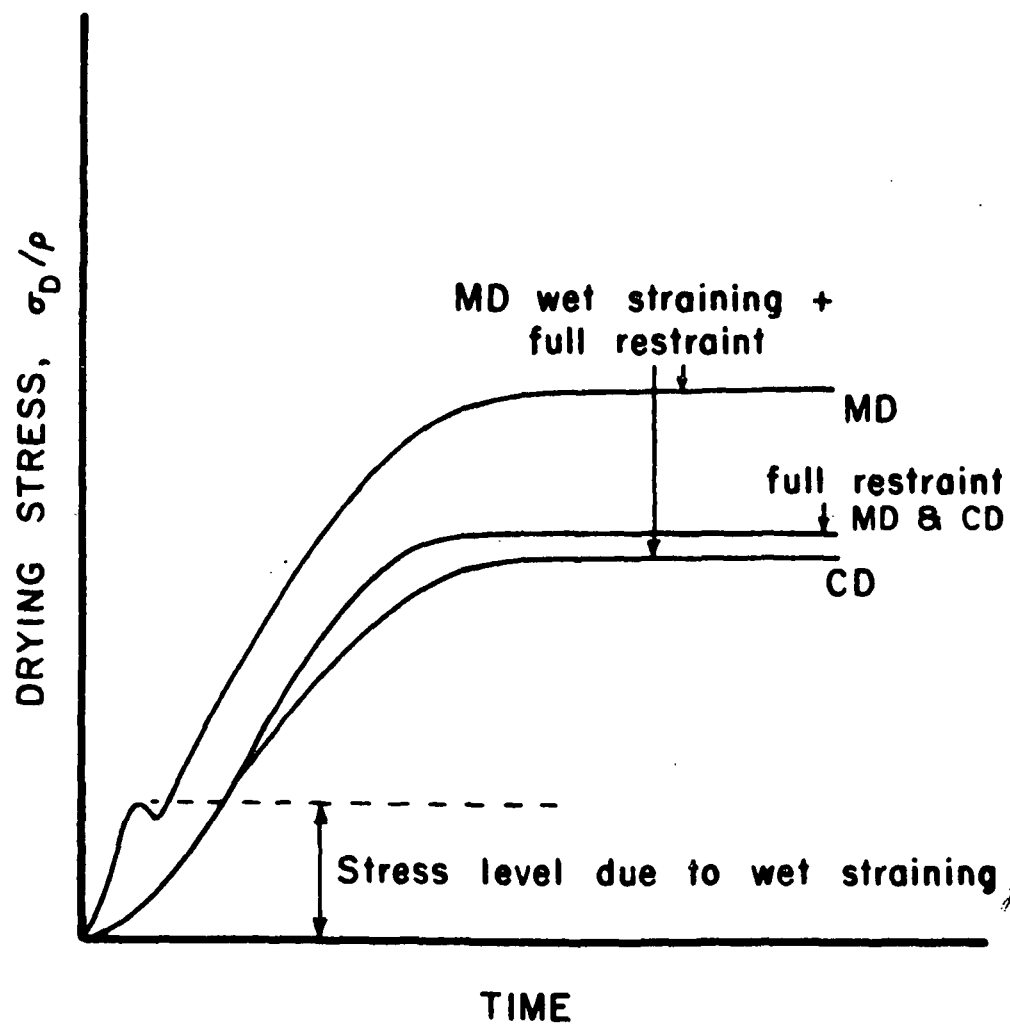
Shear mill velocity vs. laboratory shear velocity.

SECTION 3

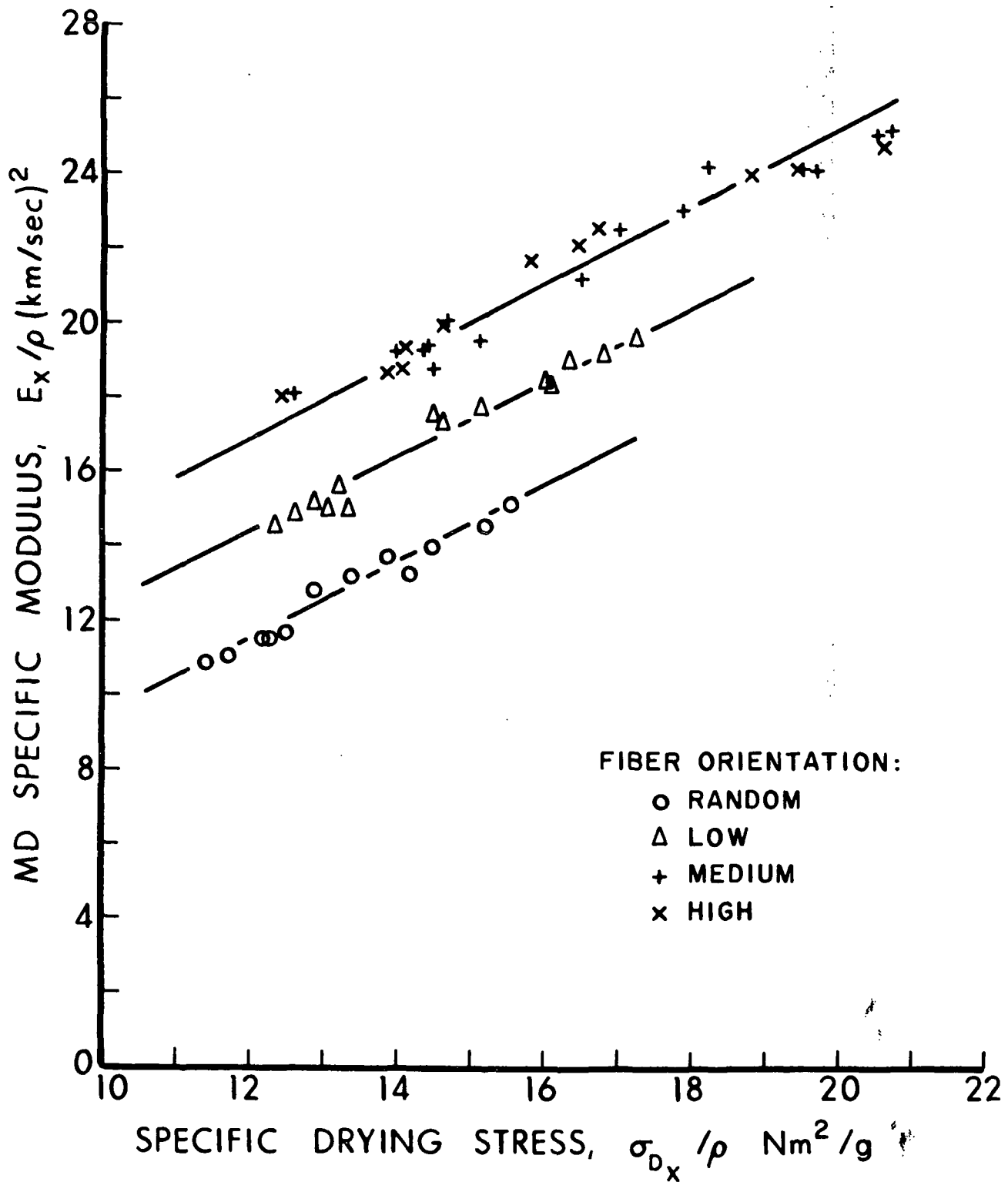
PROJECT 3500

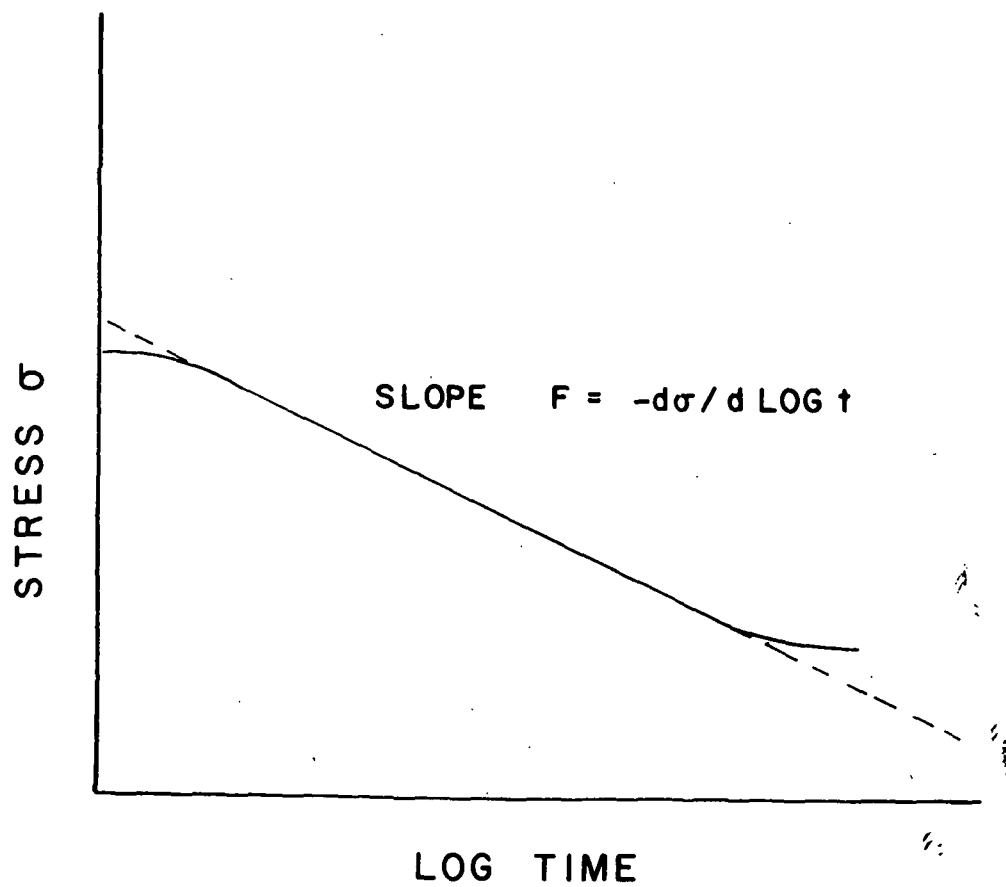
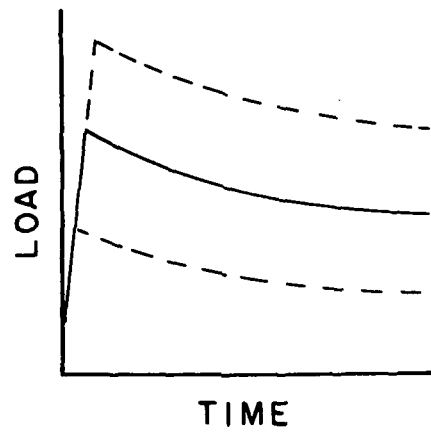
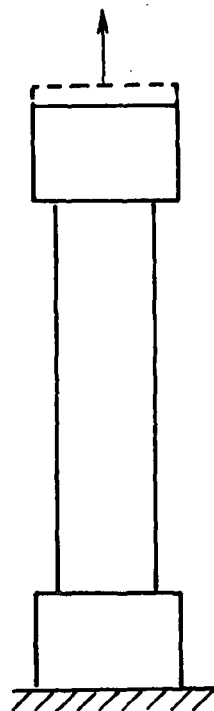
SHEAR DEFORMATION AND FAILURE

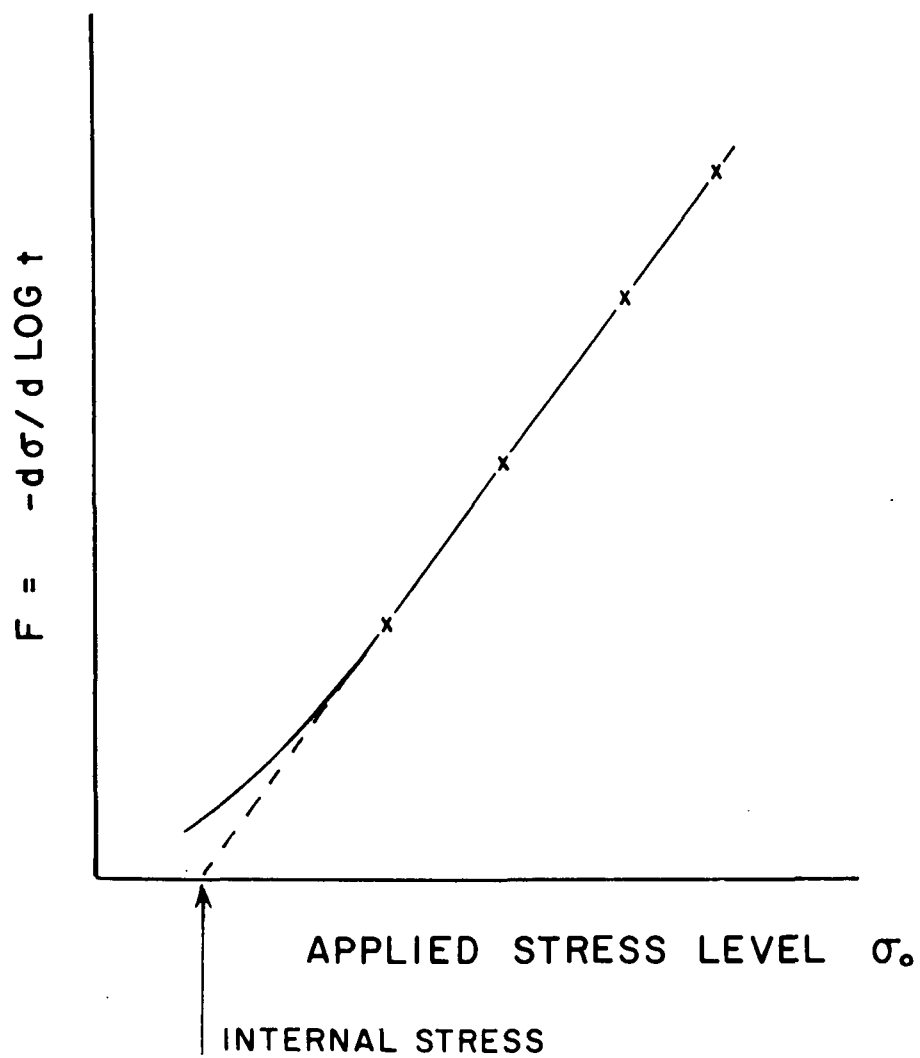
- DYNAMIC SHEAR MEASUREMENTS
- DRYING STRESS VARIATIONS IN PAPER
- RUNNABILITY OF PAPER AND BOARD

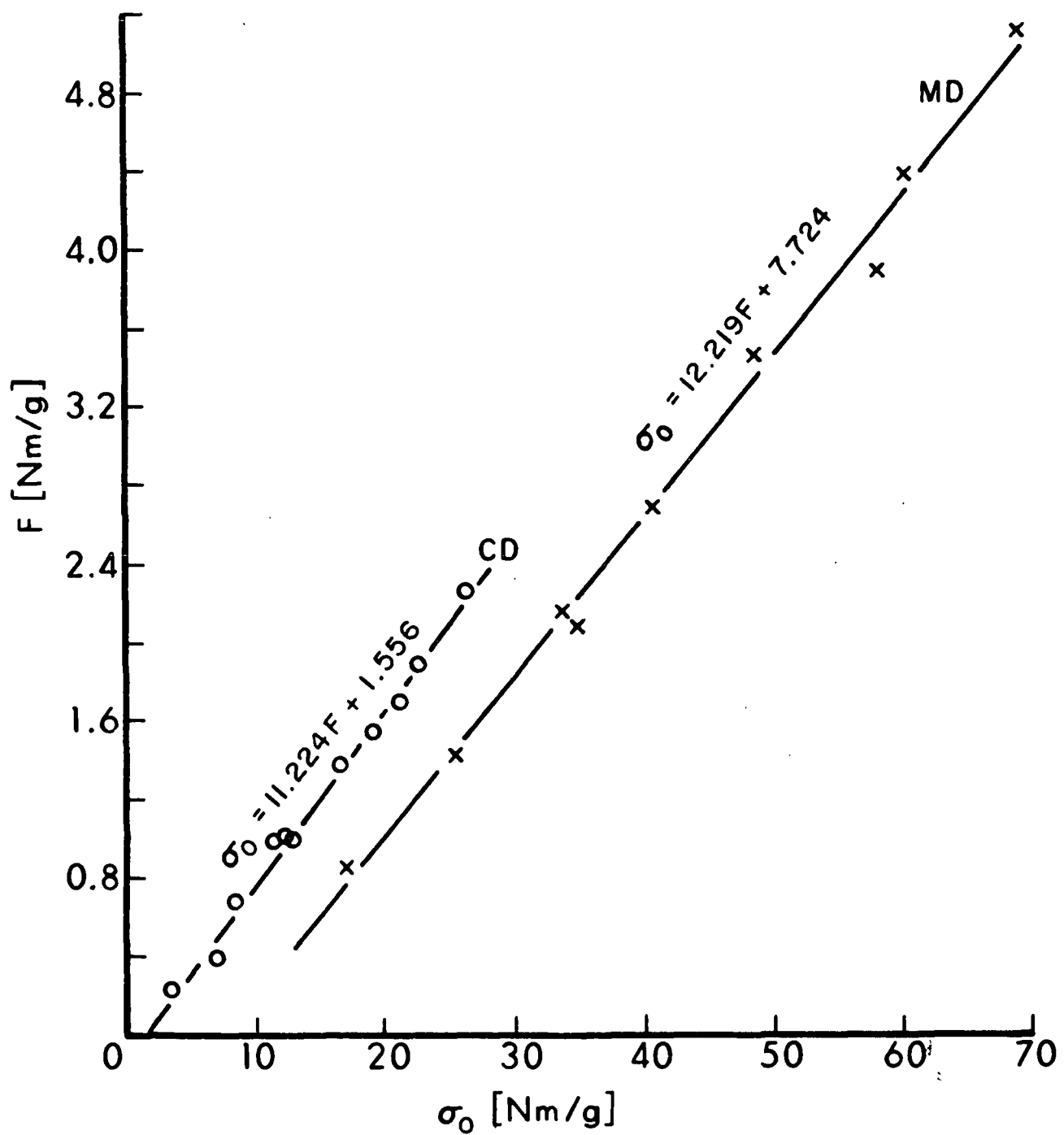


Drying stress



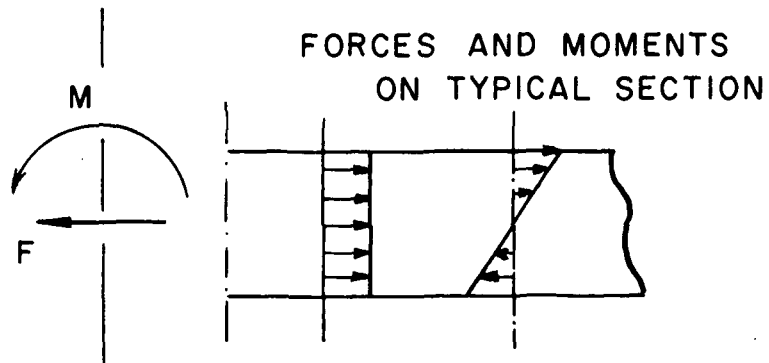


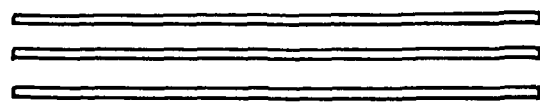


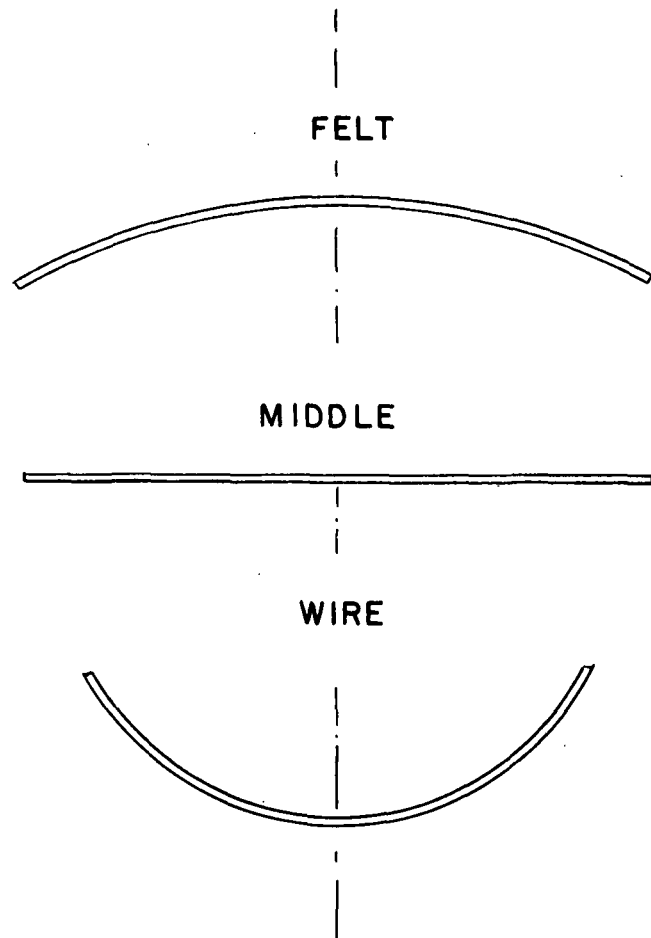


SUMMARY OF INTERNAL STRESS AND MODULUS MEASUREMENTS

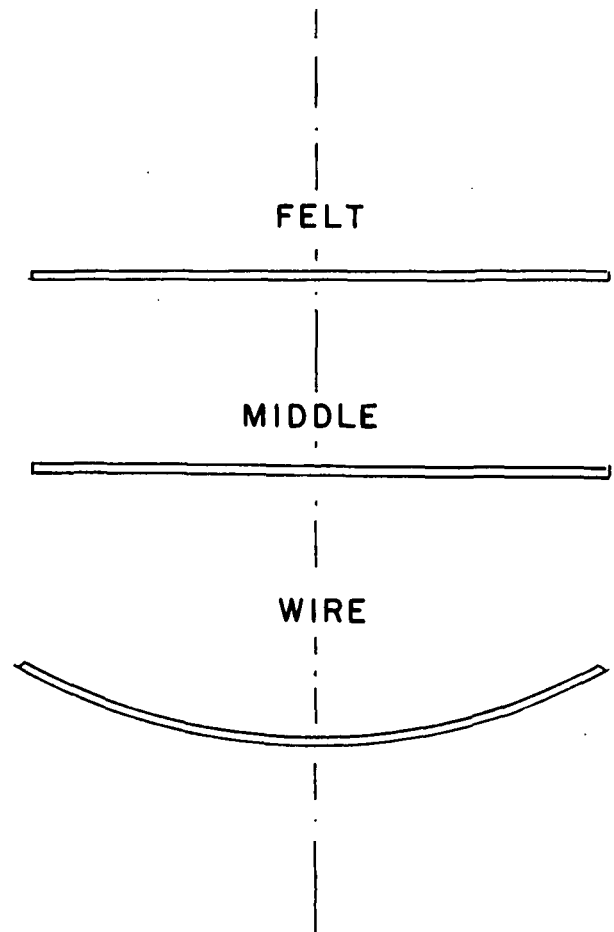
SAMPLE	INTERNAL STRESS Nm/g	E/ ρ Nm/g INSTRON	E/ ρ Nm/g ULTRASONIC
COMMERCIAL LINER MD	7.72	8.78×10^3	14.48×10^3
COMMERCIAL LINER CD	1.56	3.44×10^3	5.90×10^3
COMMERCIAL CORRUGATING MED. MD	6.12	5.52×10^3	-
COMMERCIAL CORRUGATING MED. CD	3.15	3.00×10^3	
FORMETTE HANDSHEET MD	6.60	7.24×10^3	-
FORMETTE HANDSHEET CD	3.05	3.10×10^3	




 FELT
 MIDDLE
 WIRE



CURVATURE ABOUT MD AXIS

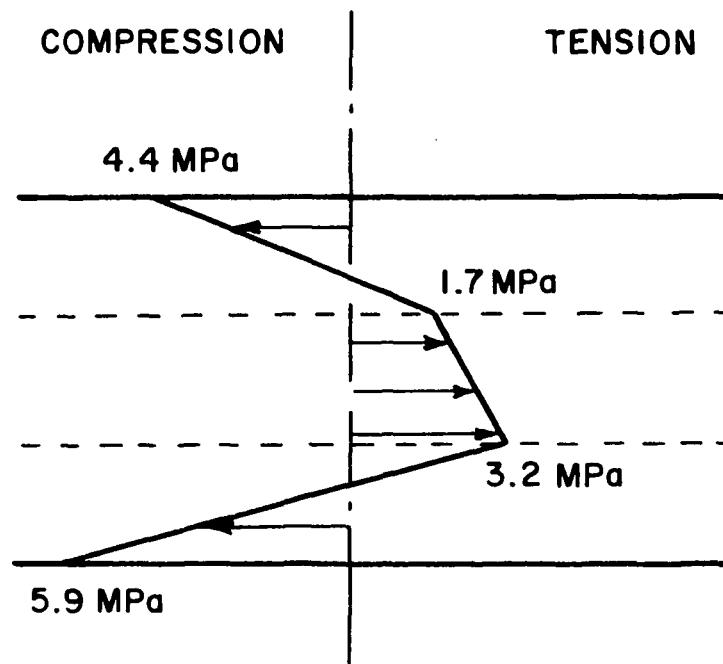


CURVATURE ABOUT CD AXIS

PROPERTIES OF SURFACE GROUND SECTION

42 lb Commercial Linerboard

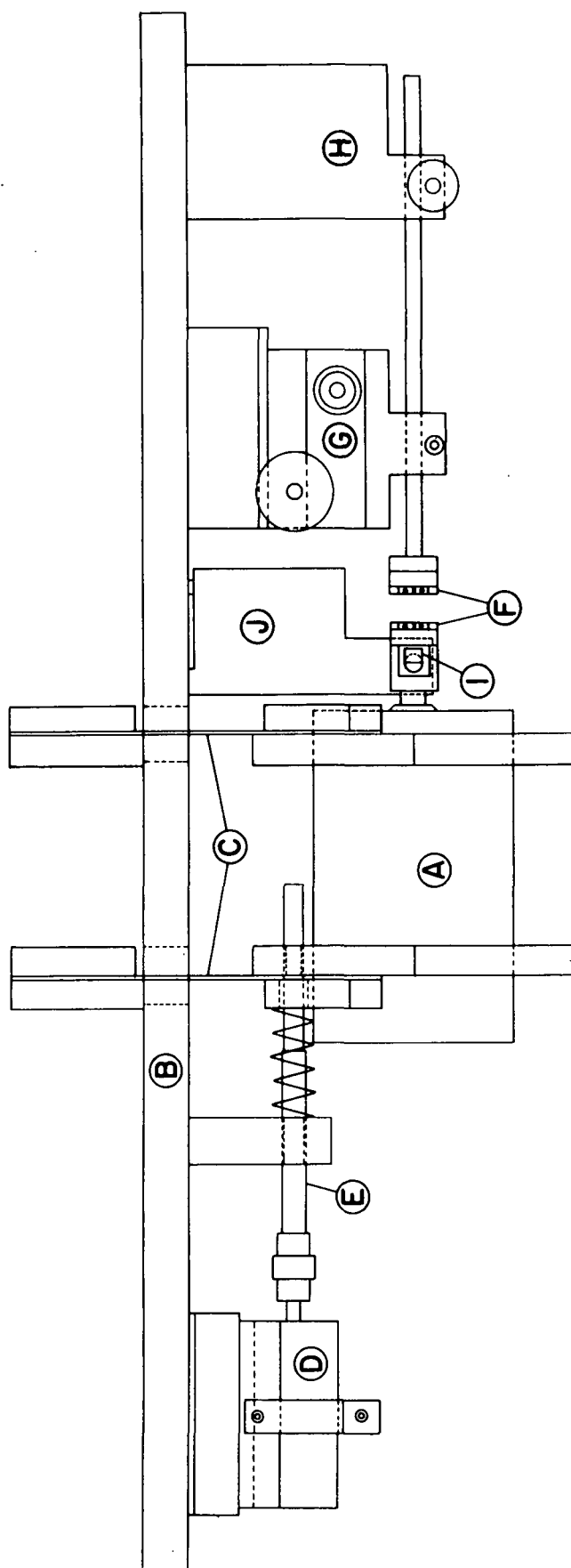
SAMPLE	BW g/m ²	IPC CAL mm	DENSITY g/cm ³	E/ρ MD (KM/sec) ²	E/ρ CD (KM/sec) ²	R	E _z /ρ (KM/sec) ²
FELT SD	94.1	0.1219	0.772	12.43 0.426	5.19 0.263	2.39	0.0692
MIDDLE SD	98.7	0.1358	0.727	11.43 0.765	5.04 0.263	2.27	0.0428
WIRE SD	86.9	0.1191	0.729	12.09 0.608	3.81 0.281	3.17	0.0595
WHOLE SHEET	207.5	0.287	0.723	13.1	6.23	2.10	0.0639



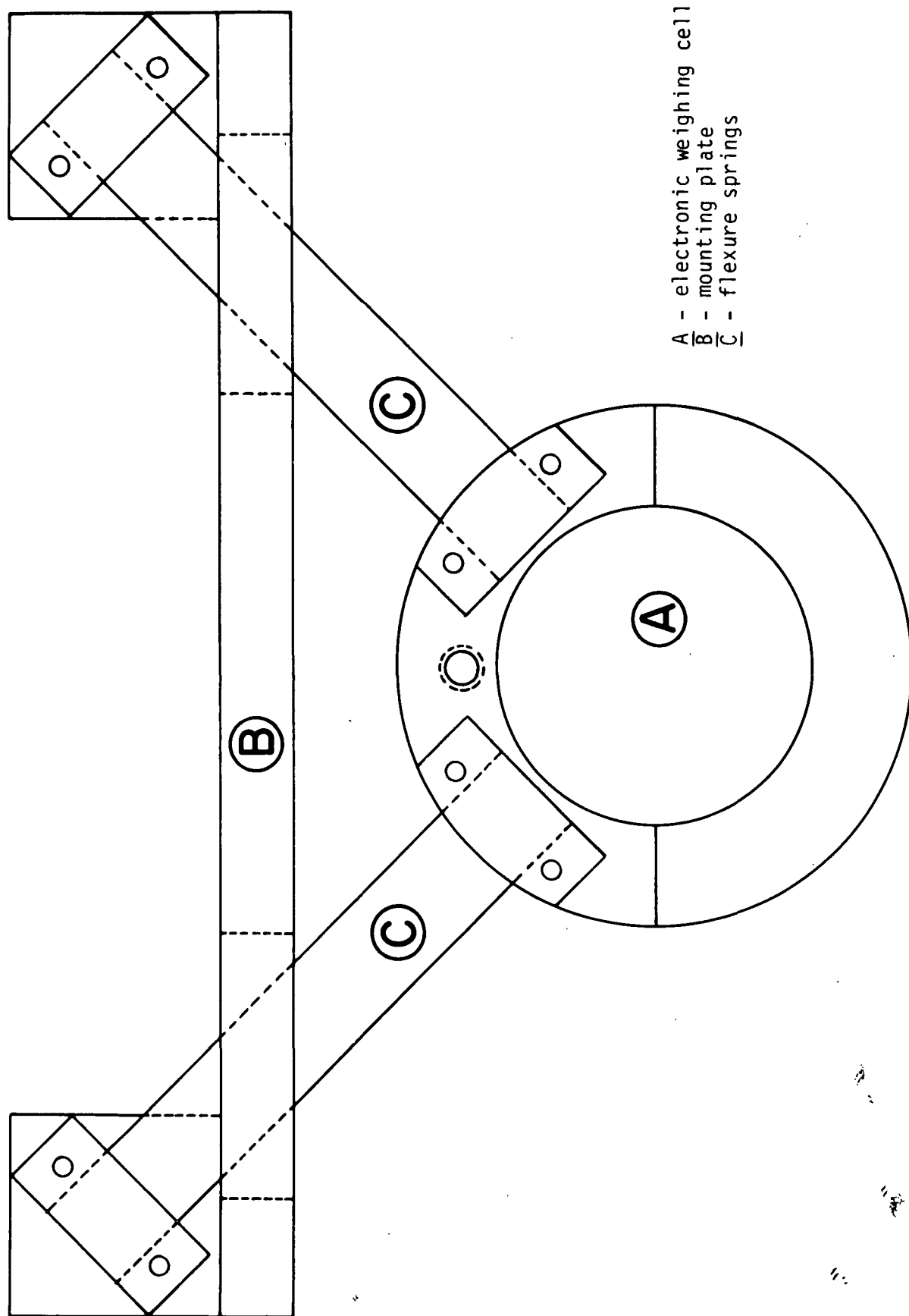
SECTION 4

PROJECT 3527

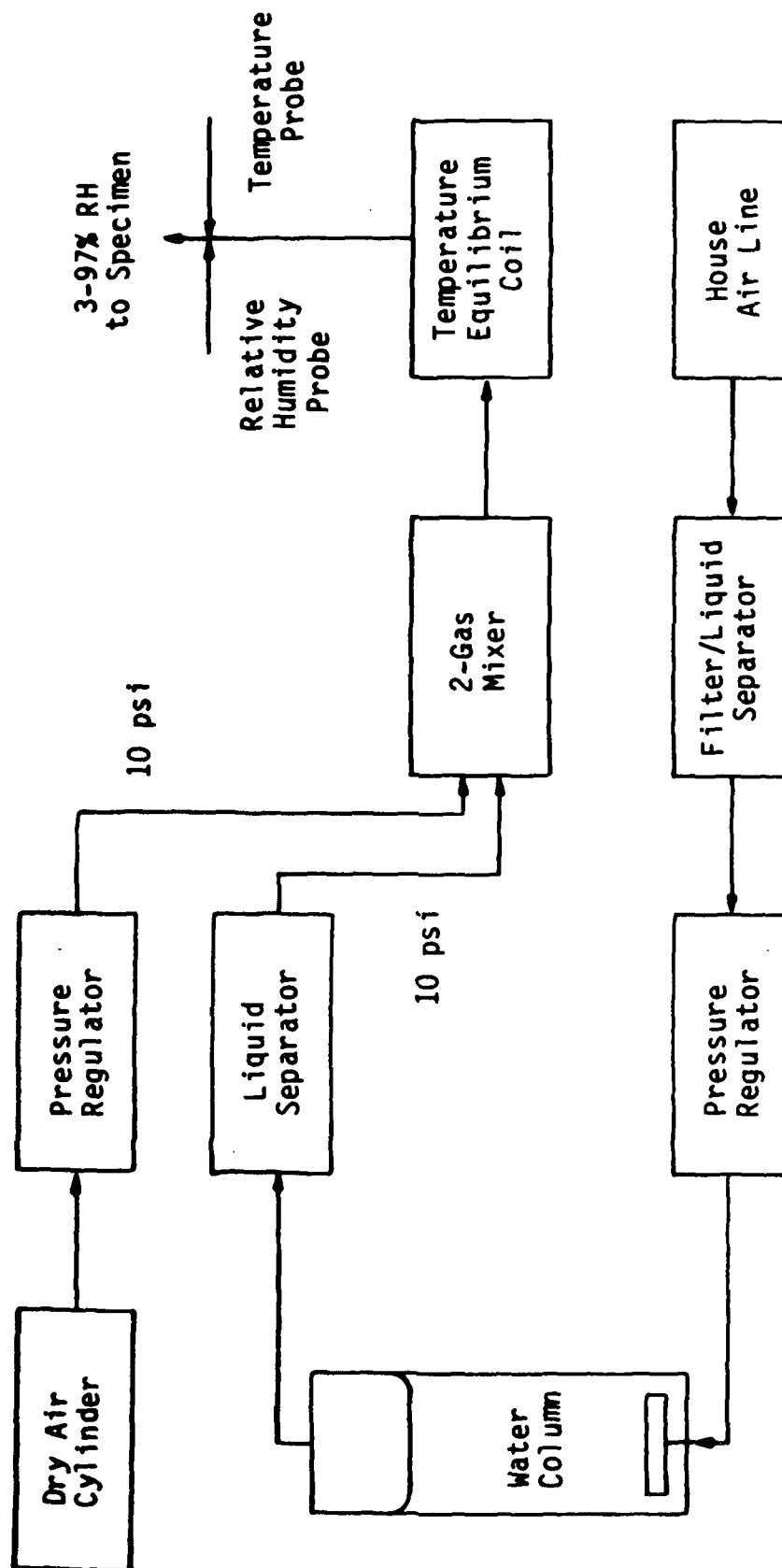
MEASUREMENT OF FIBER PROPERTIES AND FIBER-FIBER BONDING



Side view of the Fiber Load Elongation Recorder, Model II. Scale: 1 in = 5 in.
A - electronic weighing cell, B - mounting plate, C - flexure springs, D - dc
 servo motor, E - differential screw, F - clamps, G - microscope focusing
 mechanism, H - clamp, I - transducer, and J - pillar.



End view of the mounting structure for the load cell of the Fiber Load Elongation Recorder, Model II.



Concept of Specimen
Moisture Conditioner

MEASUREMENT RANGES

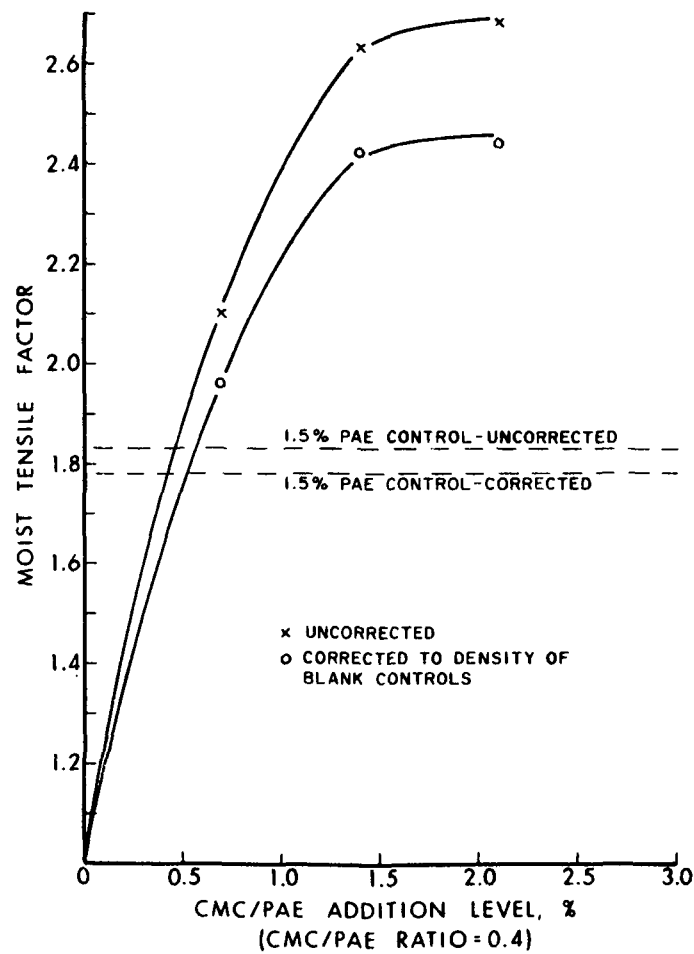
	RANGE	SENSITIVITY
LOAD CELL I	50 grams	1 milligram
LOAD CELL II	400 grams	5 milligrams
ELONGATION SENSOR I	0.05 mm	0.05 μ m
ELONGATION SENSOR II	0.25 mm	0.25 μ m
TIME TO FULL SCALE LOAD OR ELONGATION	2 sec to 400 sec	
INITIAL TEST SPAN	0 to 90 mm	

SECTION 5

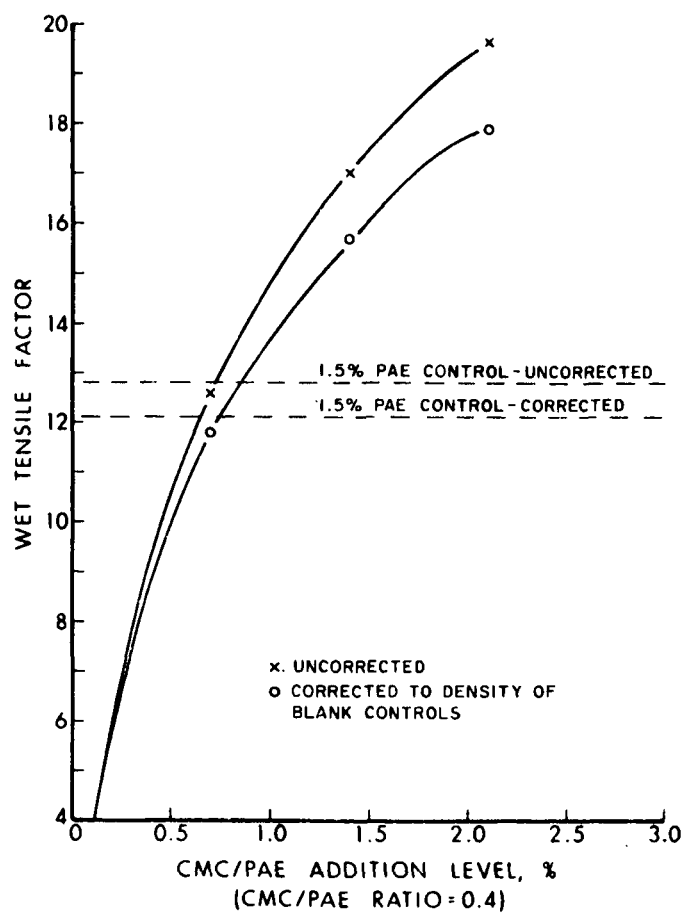
PROJECT 3526

FUNDAMENTALS OF INTERNAL STRENGTH ENHANCEMENT

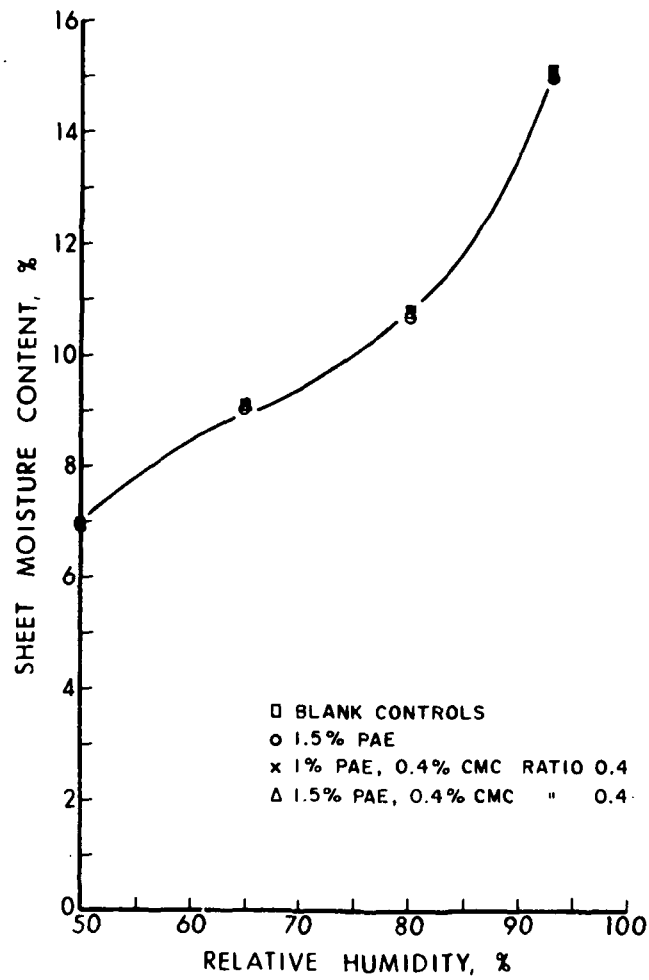
PROJECT 3526
ENHANCEMENT OF INTERNAL STRENGTH
EXPLORATORY PHASE — BONDING AGENTS



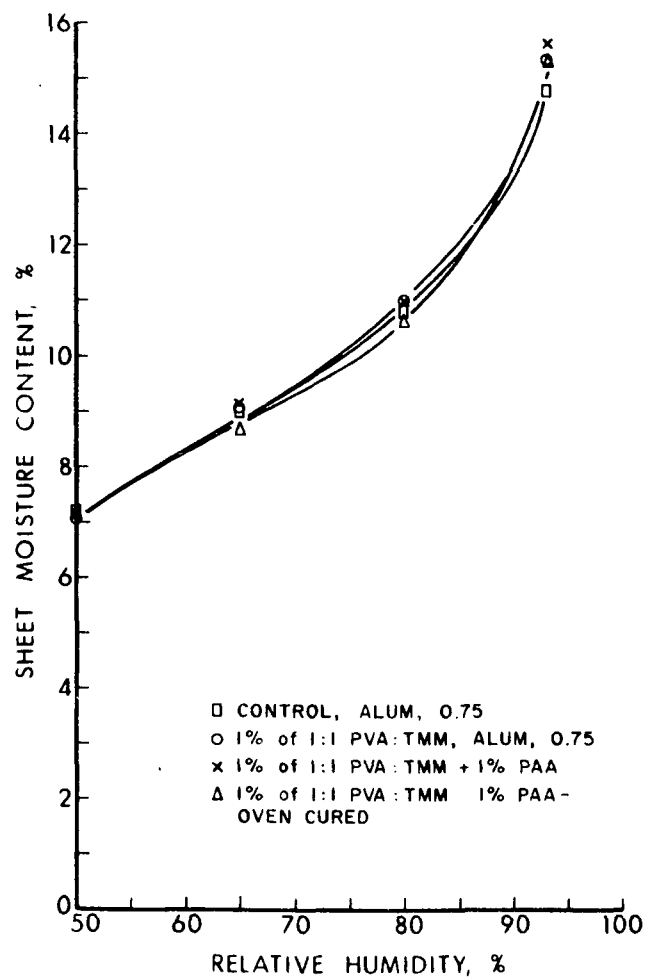
The effect of CMC/PAE addition level on moist tensile factor
(classified unbl. kraft - 48.8 yield, Kappa no. 33.7).



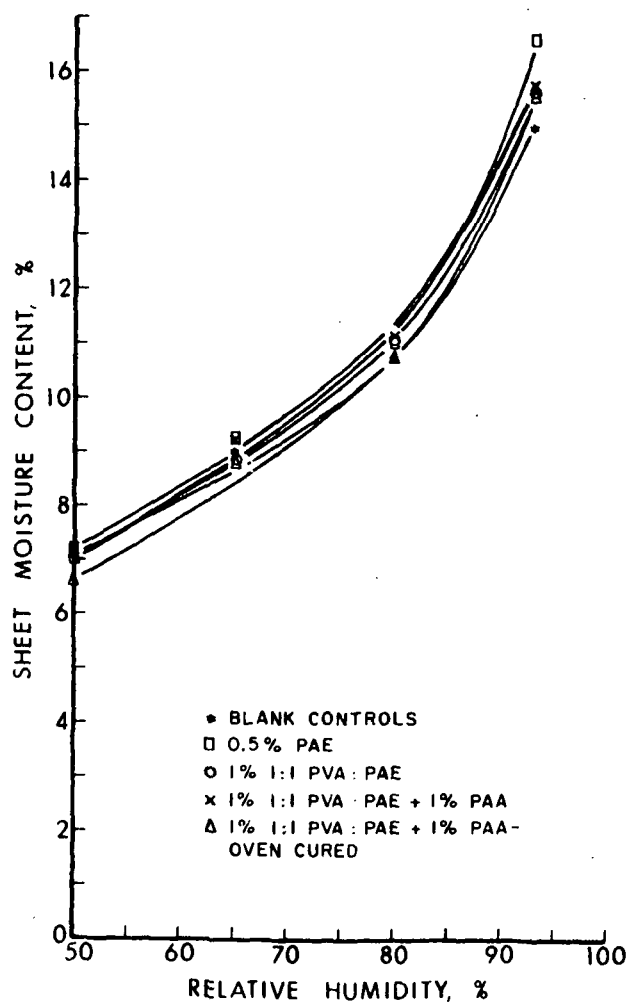
The effect of CMC/PAE addition level on wet tensile factor
(classified unbl. kraft - 48.8% yield, Kappa no. 33.7).



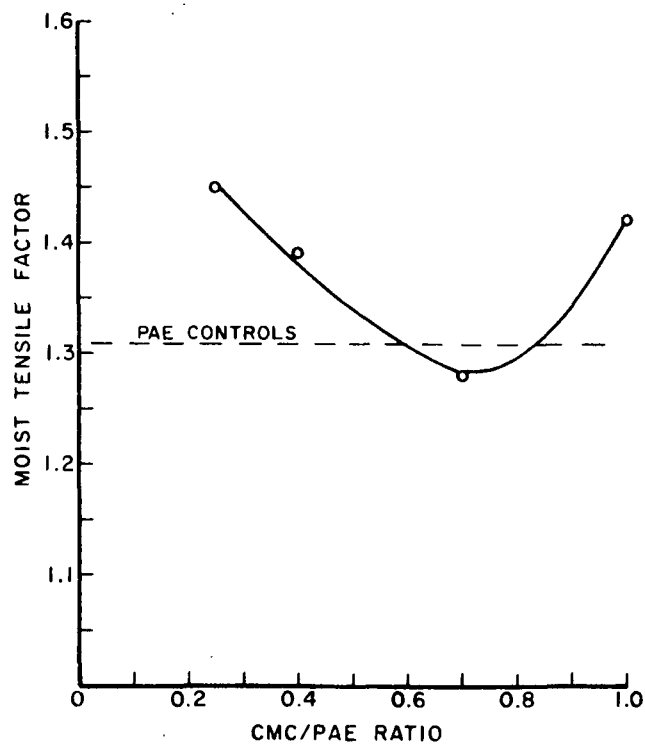
The effect of relative humidity on sheet moisture content
(classified unbl. kraft - 48.8% yield, Kappa no. 33.7;
CMC/PAE combinations).



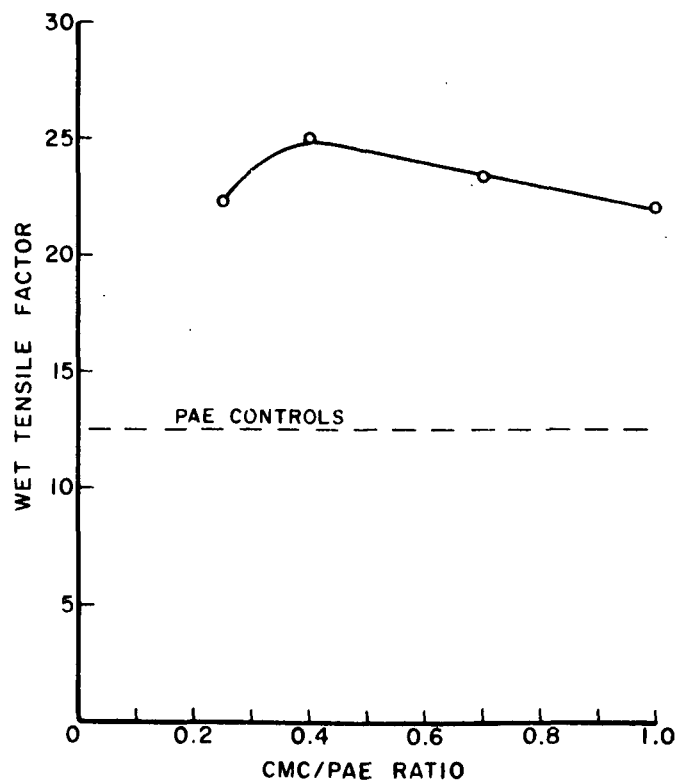
The effect of relative humidity on sheet moisture content
(classified unbl. kraft - 48.8% yield, Kappa no. 33.7;
PVA/TMM combinations).



The effect of relative humidity on sheet moisture content
(classified unbl. kraft - 48.8% yield, Kappa no. 33.7;
PVA/PAE combinations).



The effect of CMC/PAE ratio on moist tensile factor (classified unbl. kraft - 47.2% yield, Kappa no. 34.3; 1% addition).



The effect of CMC/PAE ratio on wet tensile factor (classified unbl. kraft - 47.2% yield, Kappa no. 34.3; 1% addition).

<u>Additives, % b.o.f.</u>	<u>Moist tensile factor</u>	<u>Wet tensile factor</u>	<u>Sizing, sec.</u>
PAE, 1.0; CMC, 0.4	2.57	20.7	0
PAE, 1.0; CMC, 0.4 Rosin size, 0.5	2.35	20.3	1800+
PAE, 1.0; CMC, 0.4 Synthetic size, 0.25	2.48	16.7	1800+

UNCLASSIFIED PULP

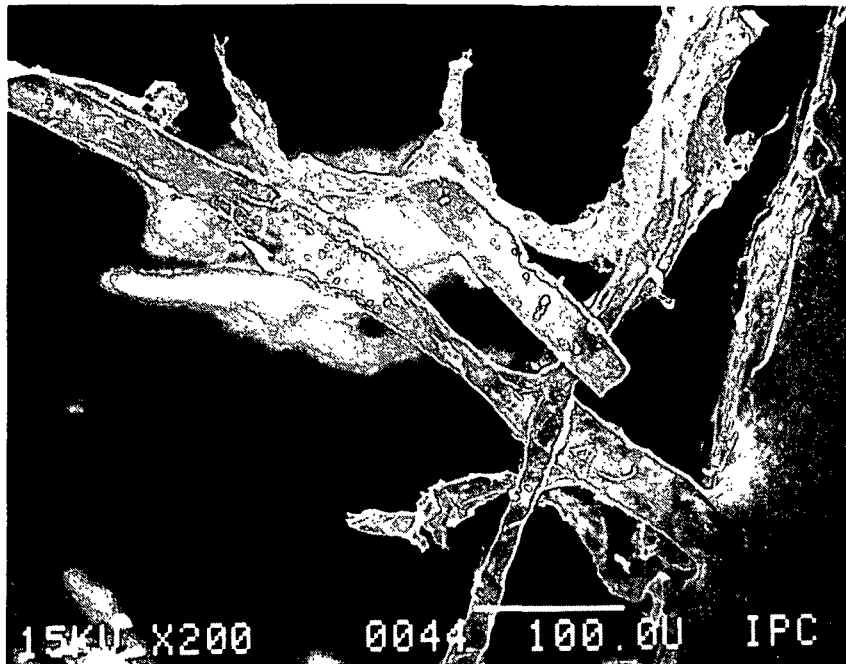
<u>Additives, % b.o.f.</u>	<u>Moist tensile factor</u>	<u>Wet tensile factor</u>
PAE, 1.0	1.60	10.3
PAE, 1.0; CMC, 0.4	1.80	11.1
1:1 PVA:PAE, 1.0 + PAA, 1.0	1.86	12.0

CLASSIFIED PULP

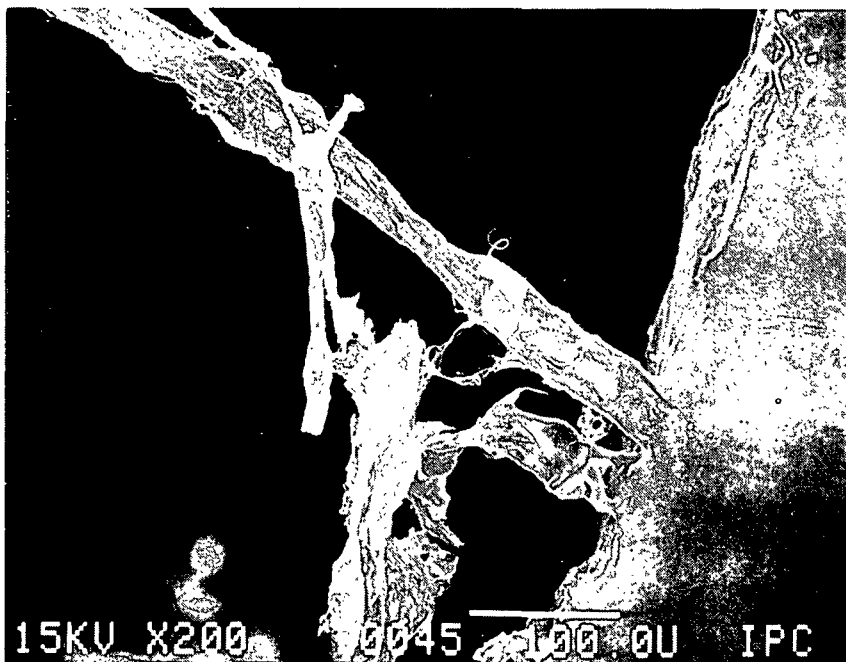
<u>Additives, % b.o.f.</u>	<u>Moist tensile factor</u>	<u>Wet tensile factor</u>
PAE, 1.0	1.31	12.5
PAE, 1.0; CMC, 0.4	2.57	20.7
1:1 PVA:PAE, 1.0 + PAA, 1.0	2.61	15.2

FUTURE WORK

1. Chemical analysis of treated papers to determine polymer retention and, if feasible, configuration of retained species.
2. Continued studies of polymeric additives and paper repulpability.
3. Efficiency of multicomponent systems in high-yield pulps.
4. New approaches for improving the moisture tolerance of paper.

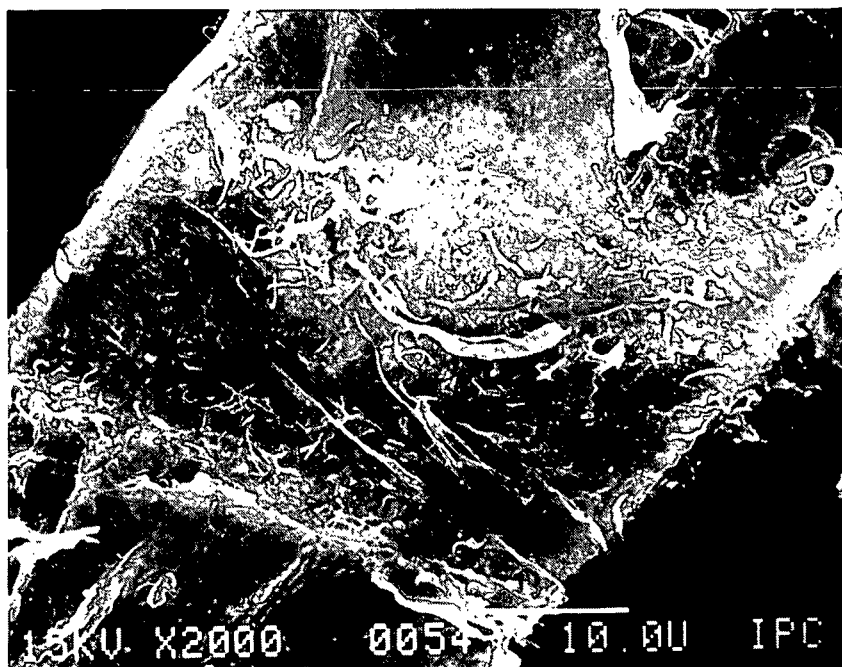


a)

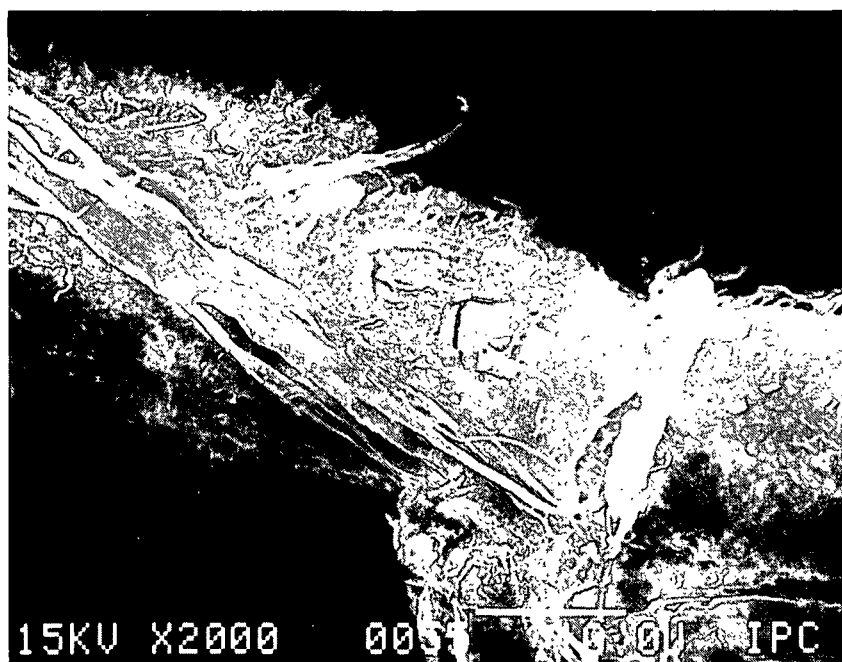


b)

- a) Fiber/fiber bond before straining. Refined southern pine.
b) After straining. Note charging on Fiber No. 2 indicating formerly bonded area.

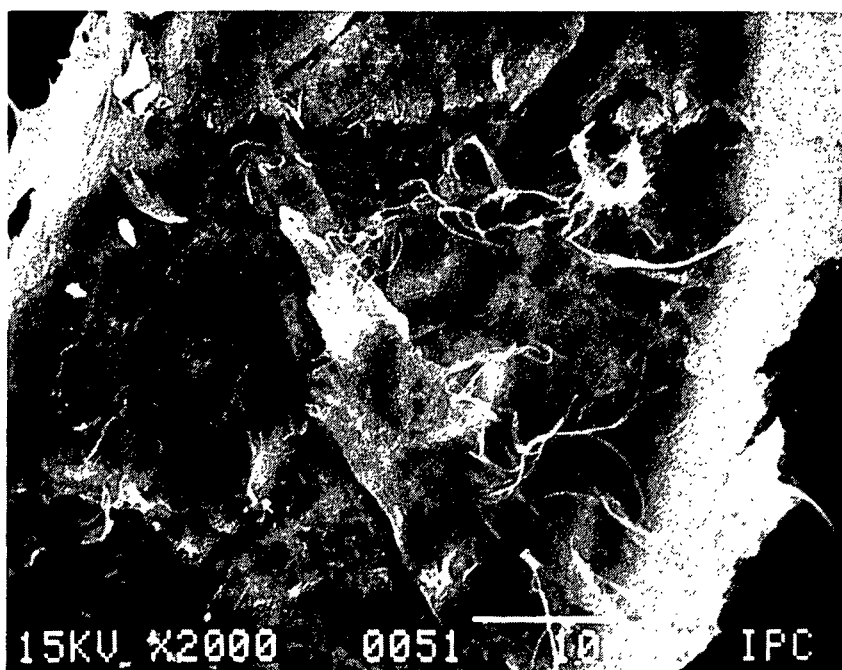


a)



b)

Same fibers as previous page shown after coating with aluminum.
a) Fiber No. 2, b) Fiber No. 1



Failed bond of refined southern pine showing disruption of fiber surface along periphery of formerly bonded area.

STRENGTH OF FIBER/FIBER BONDS†

Fiber	Force at failure, g	Fiber	Force at failure, g
Springwood	0.48	Summerwood	0.63
Springwood	0.13	Summerwood	0.08
Springwood	0.61	Summerwood	0.04
Springwood	0.17	Summerwood	1.30
		Summerwood	0.57
Refined	0.59	Summerwood	0.48
Refined	0.12*	Summerwood	0.72

†Dried under pressure

STRENGTH OF FIBER/FIBER BONDS†

Fiber	Force at failure, g
Summerwood	0.55
Summerwood	0.45
Summerwood	0.33
Summerwood	0.54
Summerwood	0.02
Refined	0.52
Refined	0.69
Refined	0.90
Refined	1.68*
Refined	1.28*

†Dried under pressure

SECTION 6

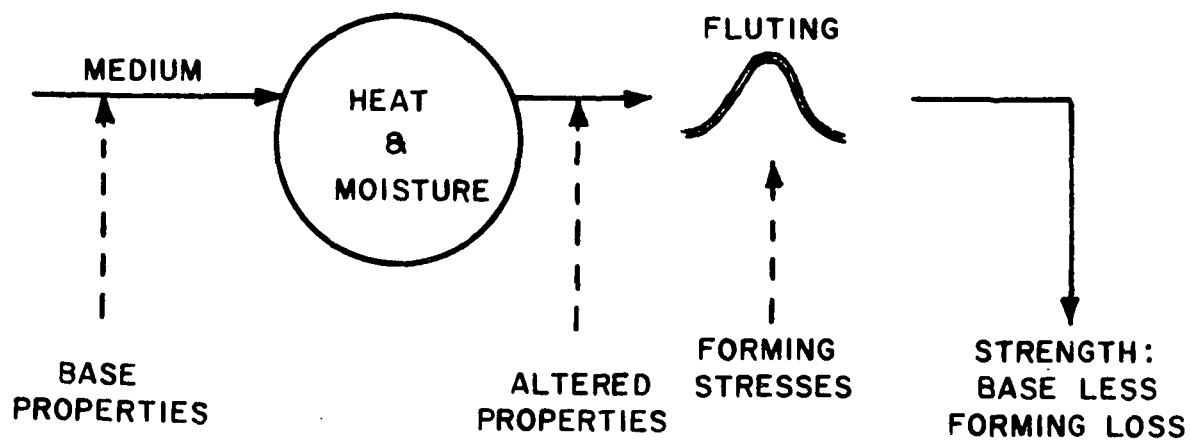
PROJECT 3396

MECHANICS OF FLUTING

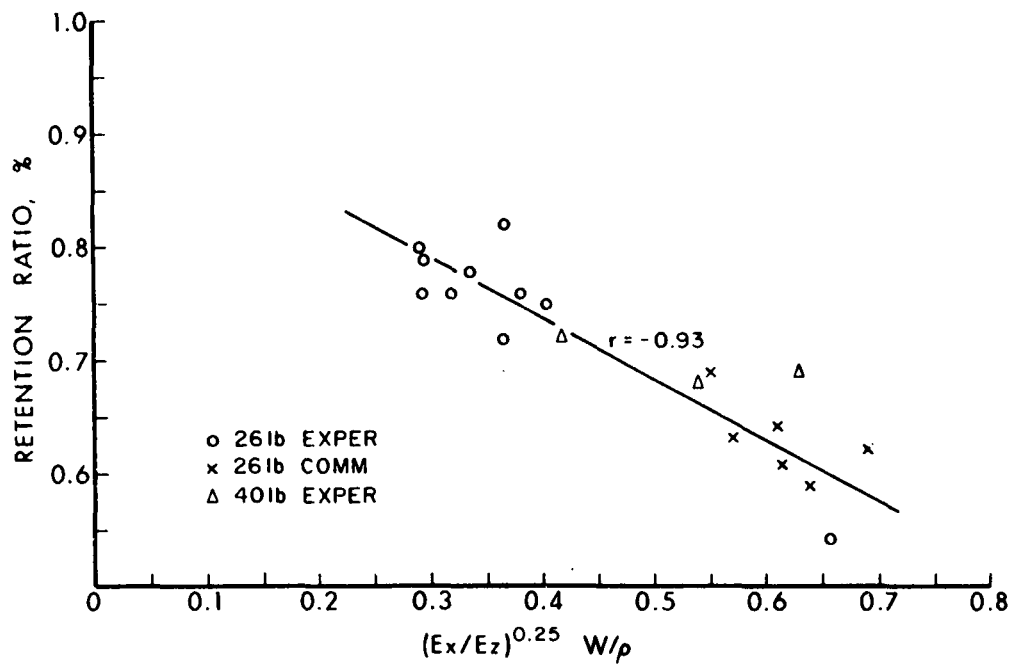
MECHANICS OF FLUTING

CORRUGATING MEDIUM GOALS

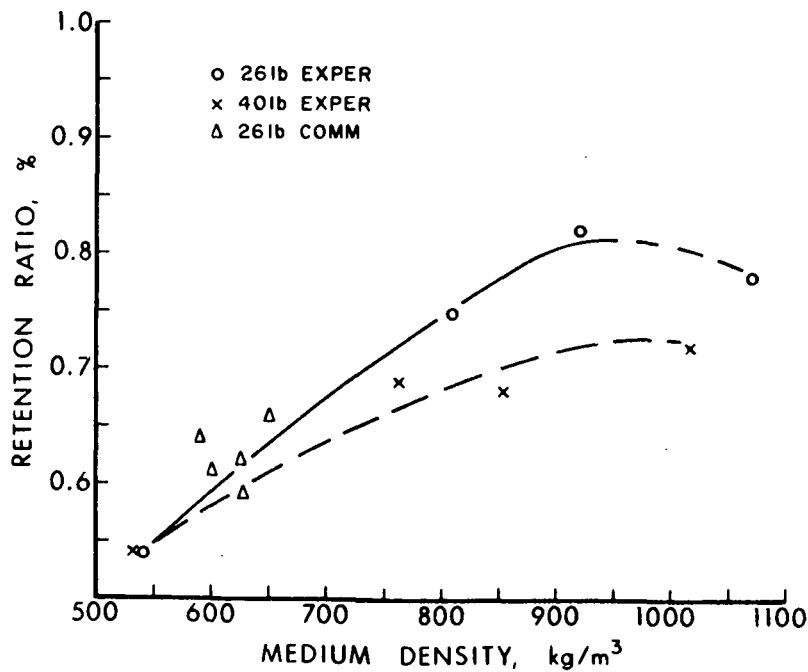
- IMPROVED END-USE COST/PERFORMANCE
- MAINTAIN OR IMPROVE FORMABILITY



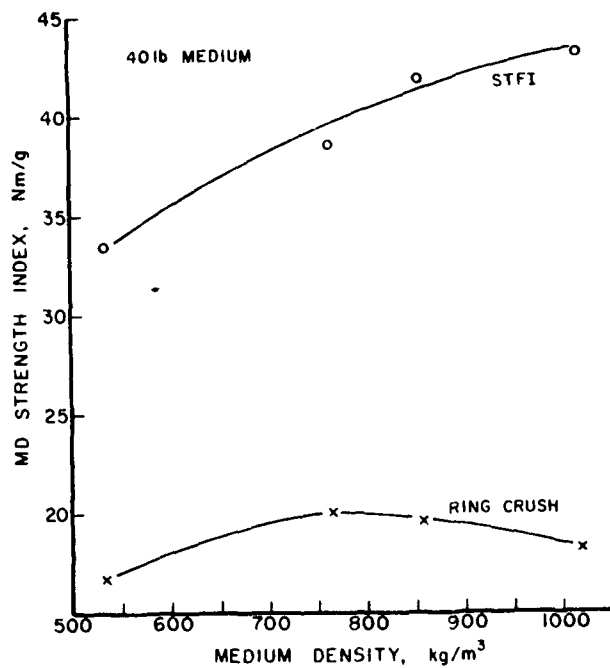
Schematic of forming process.



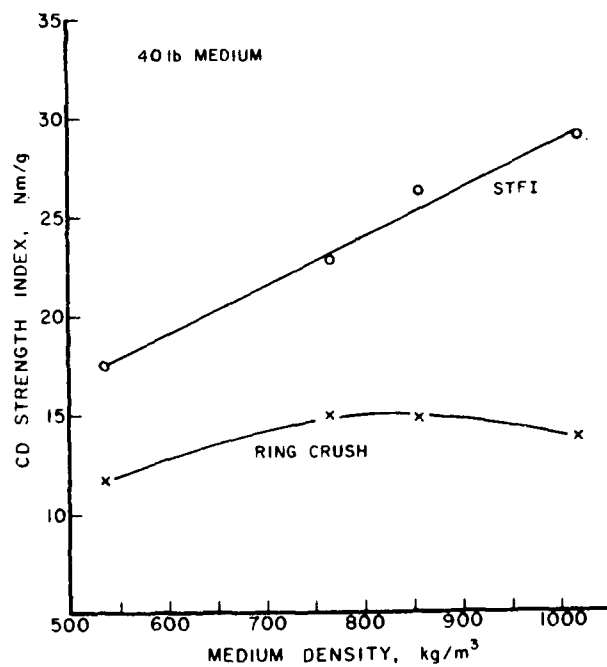
Retention of compressive strength during fluting depends on elastic stiffnesses, (E_x/E_z) basis weight (W) and density (ρ).



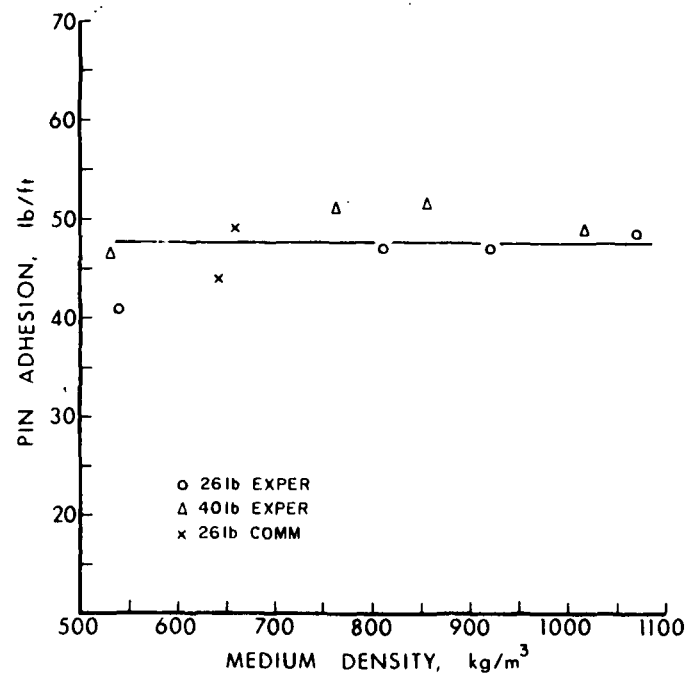
Effect of density on retention of compressive strength during fluting.



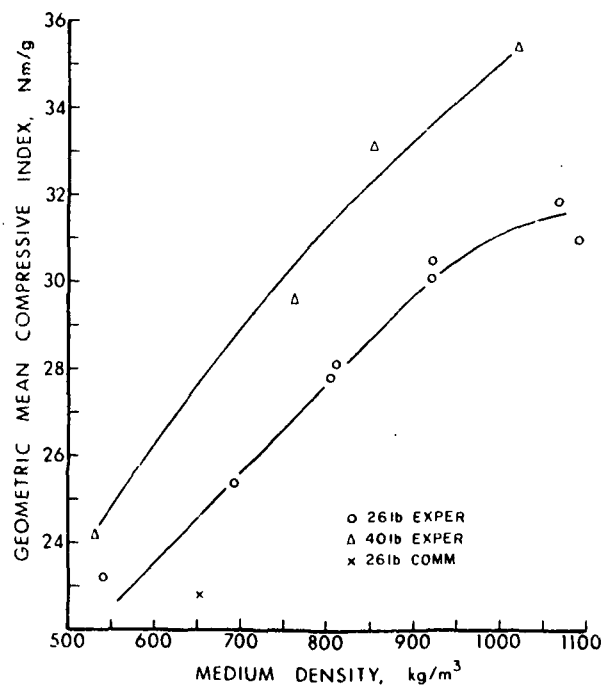
MD STFI and ring crush show different trends with increasing medium density.



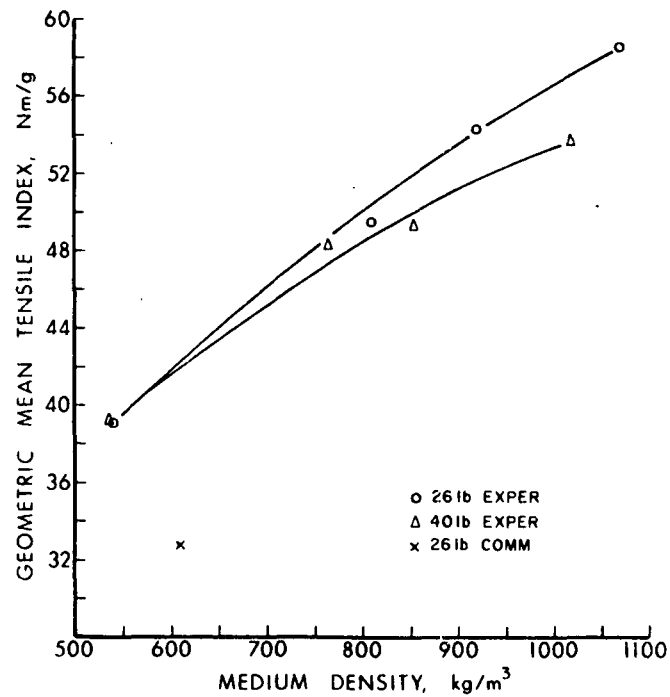
CD STFI and ring crush show different trends with increasing medium density.



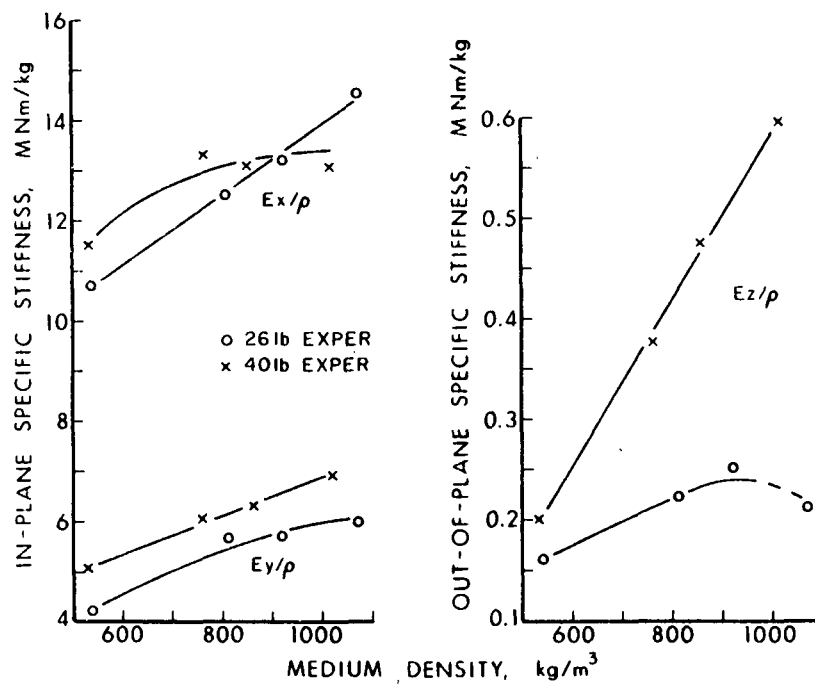
Single-face pin adhesion results in experimental and commercial mediums.



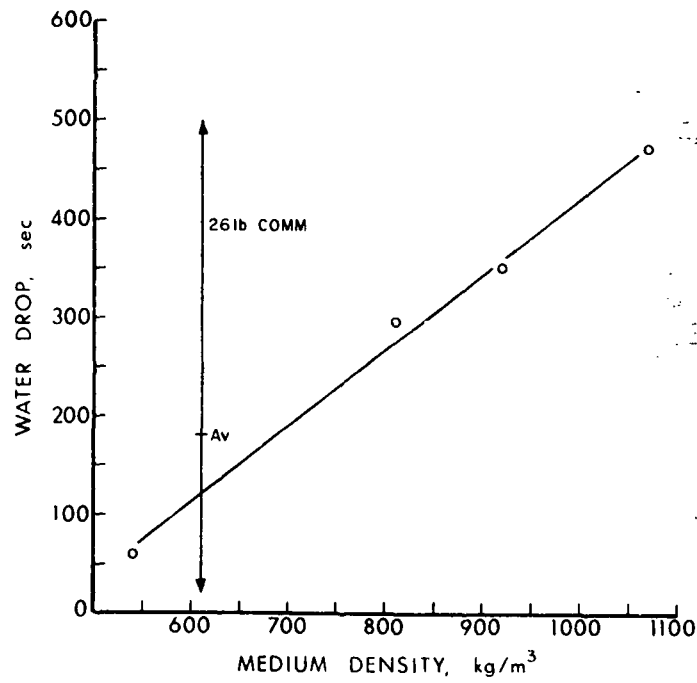
Geometric mean compressive index increases as density increases.



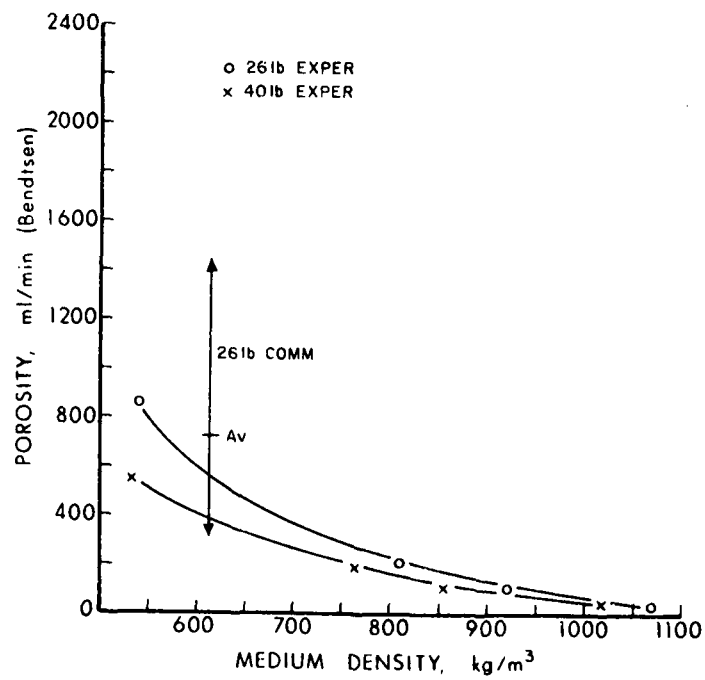
Increased wet pressing increases tensile strength.



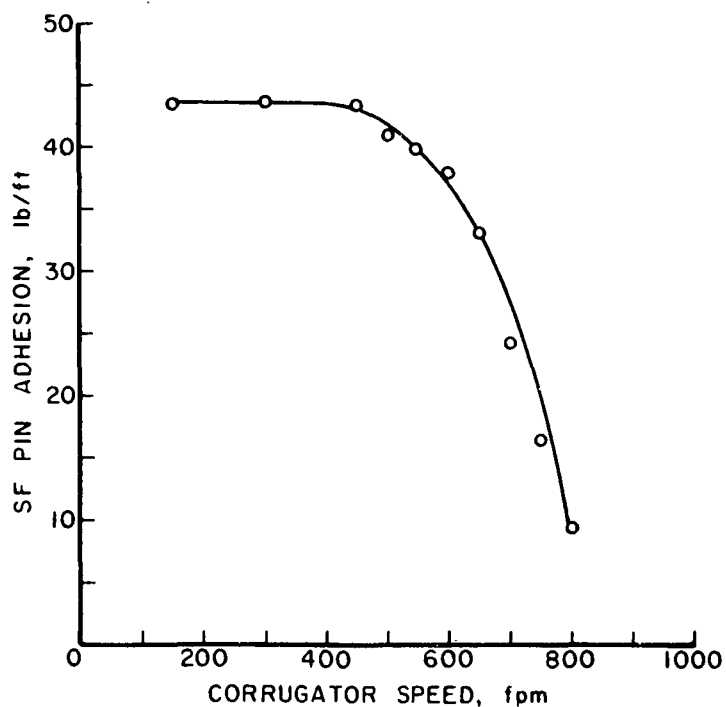
Effect of density on elastic stiffnesses.



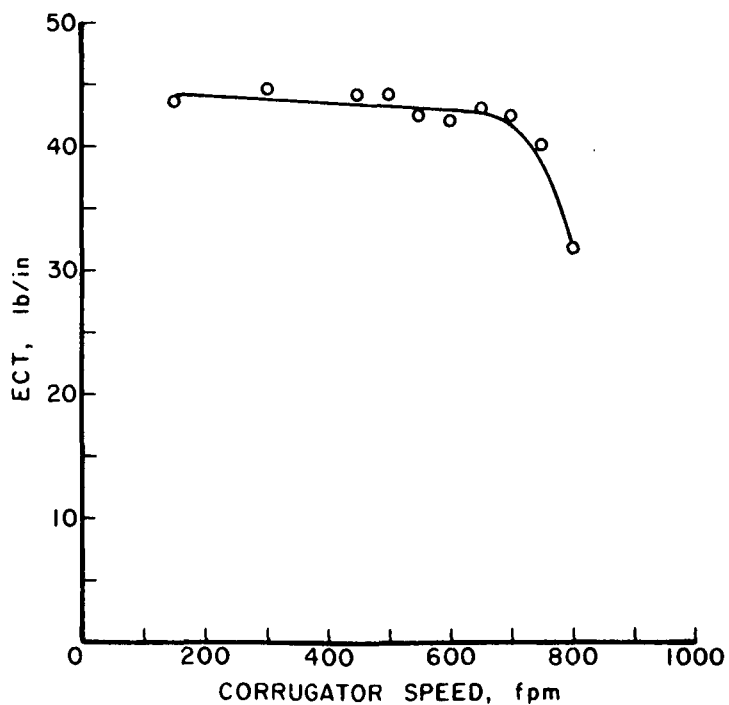
Effect of density on medium water receptivity.



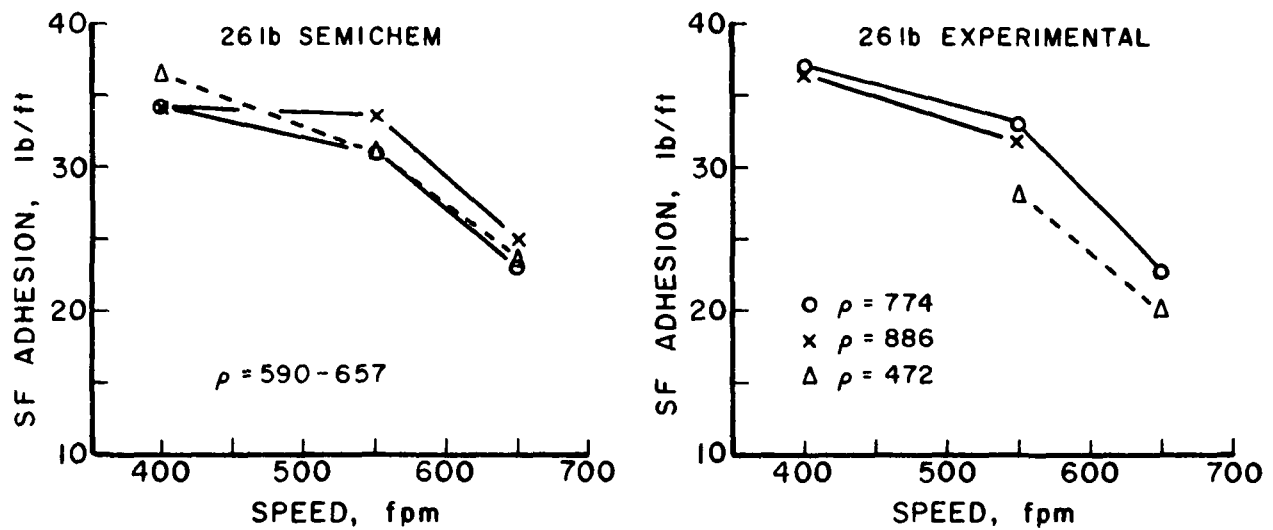
Effect of medium density on porosity.



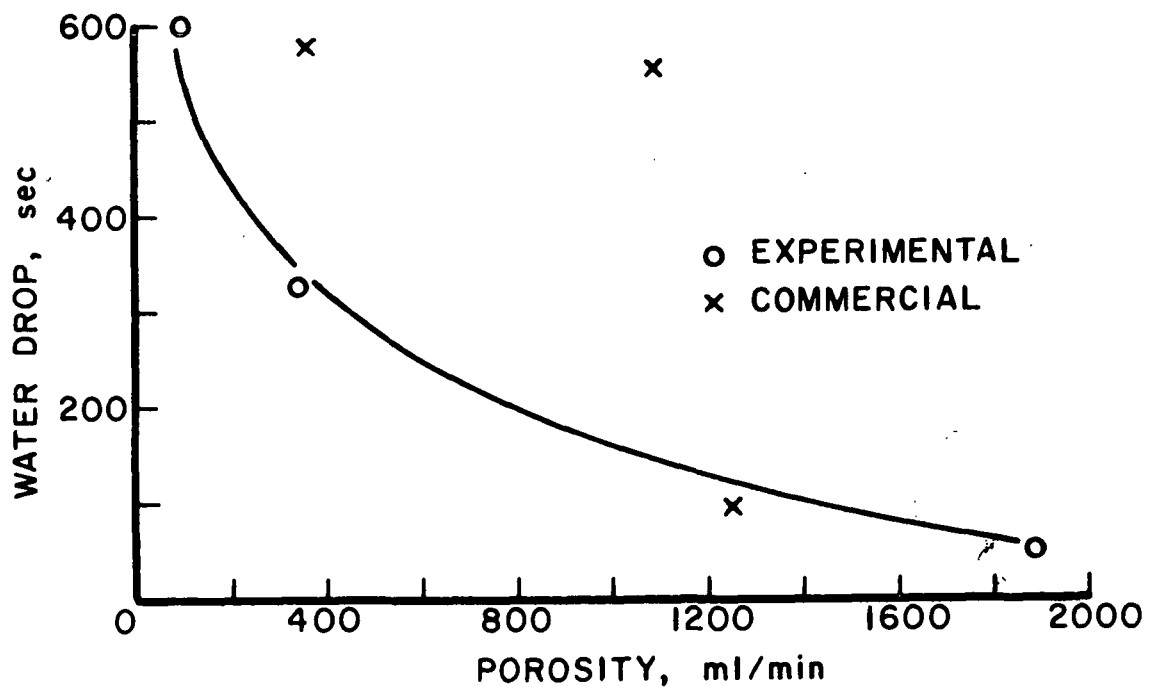
Effect of corrugating speed on pin adhesion for 26 lb commercial medium combined with 42 lb liner.



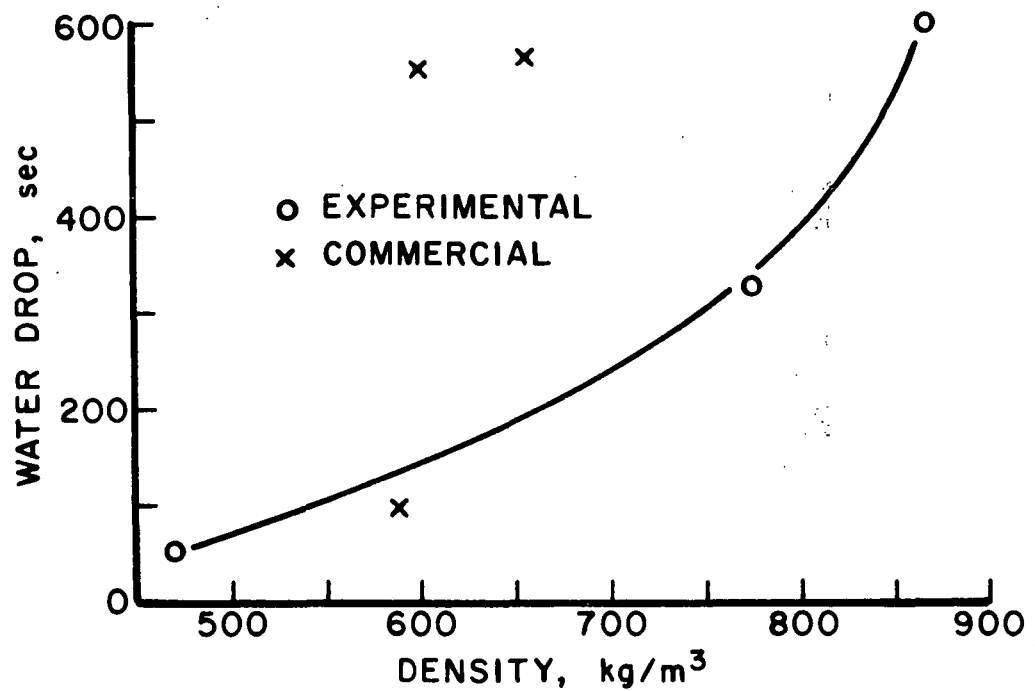
Effect of corrugating speed on ECT for 26 lb commercial medium combined with 42 lb liner.



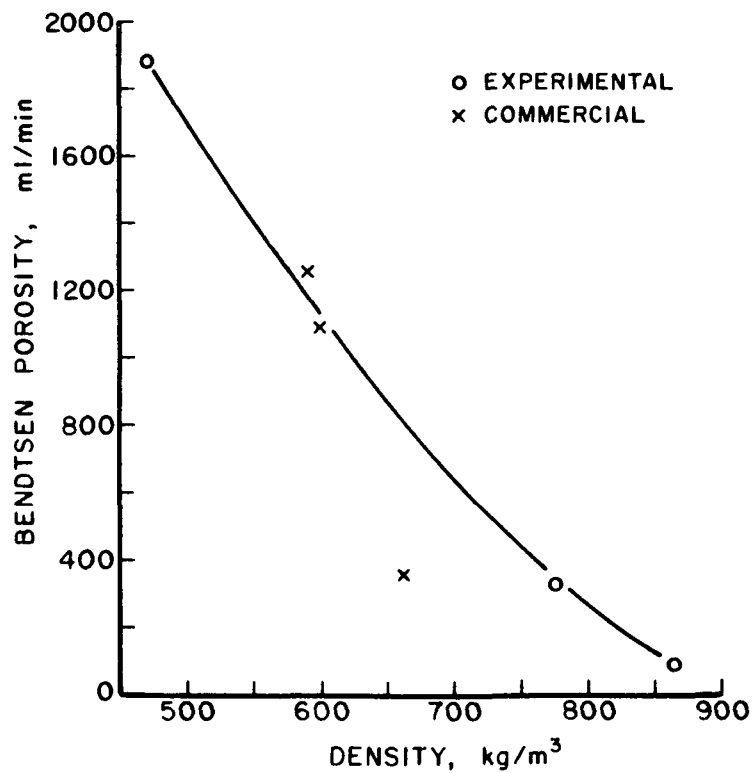
Comparison of single-face adhesion results on commercial and experimental densified mediums.



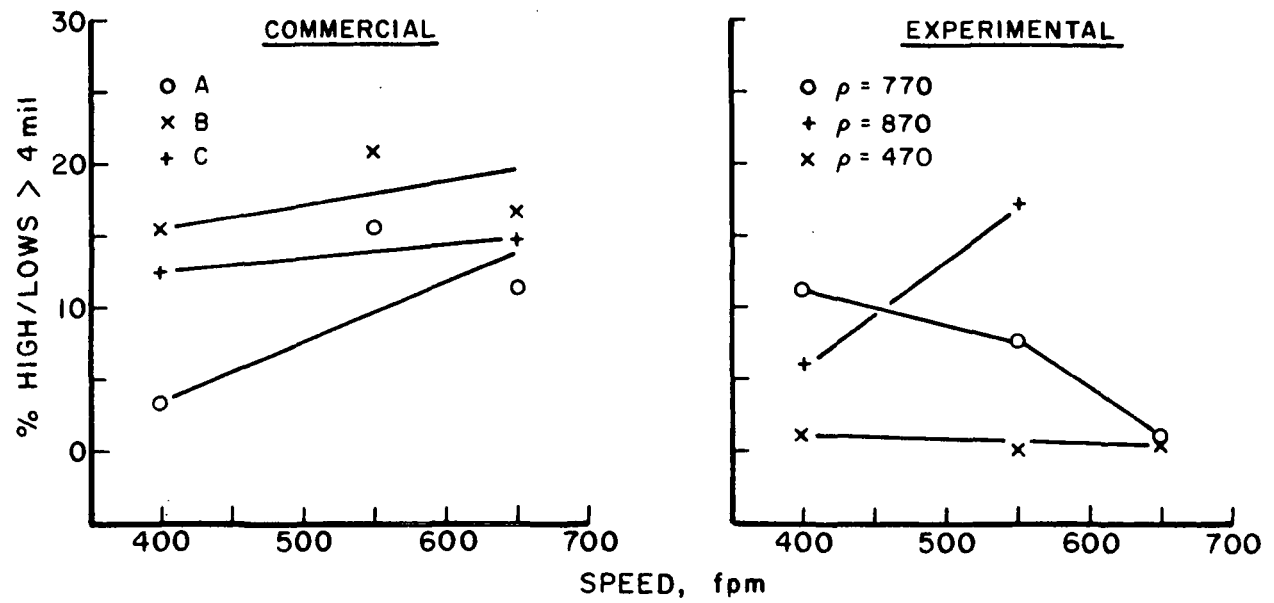
Comparison of water drops vs. porosity results on commercial and experimental mediums.



Effect of densification in water drop results (with commercial control results for comparison).



Effect of densification on porosity (with commercial control results for comparison).



High/low results on commercial and densified mediums.

SECTION 7

PROJECT 3469

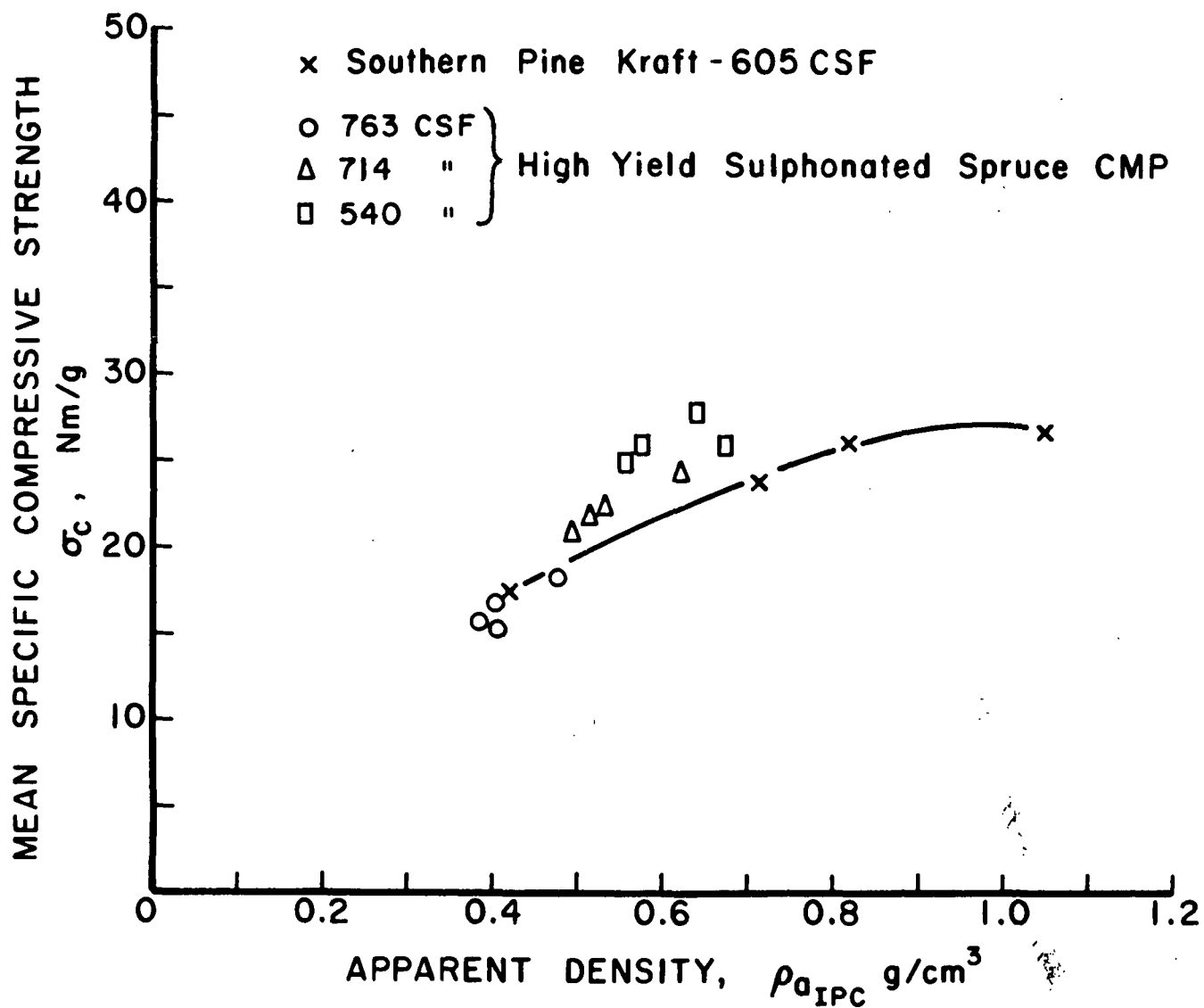
COMPRESSIVE STRENGTH

RAW MATERIALS

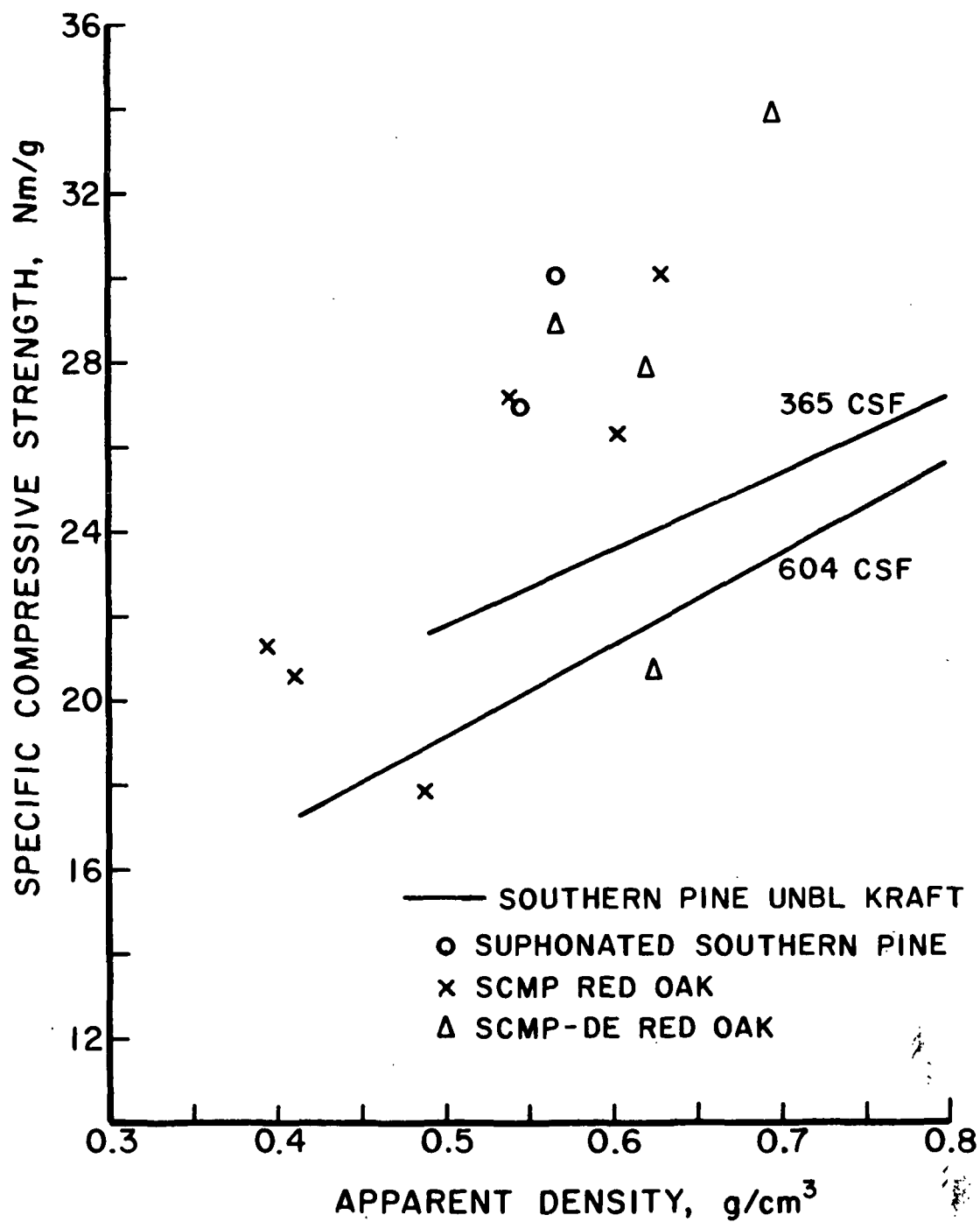
- HIGH YIELD PULPS
- POLYMER REINFORCEMENT

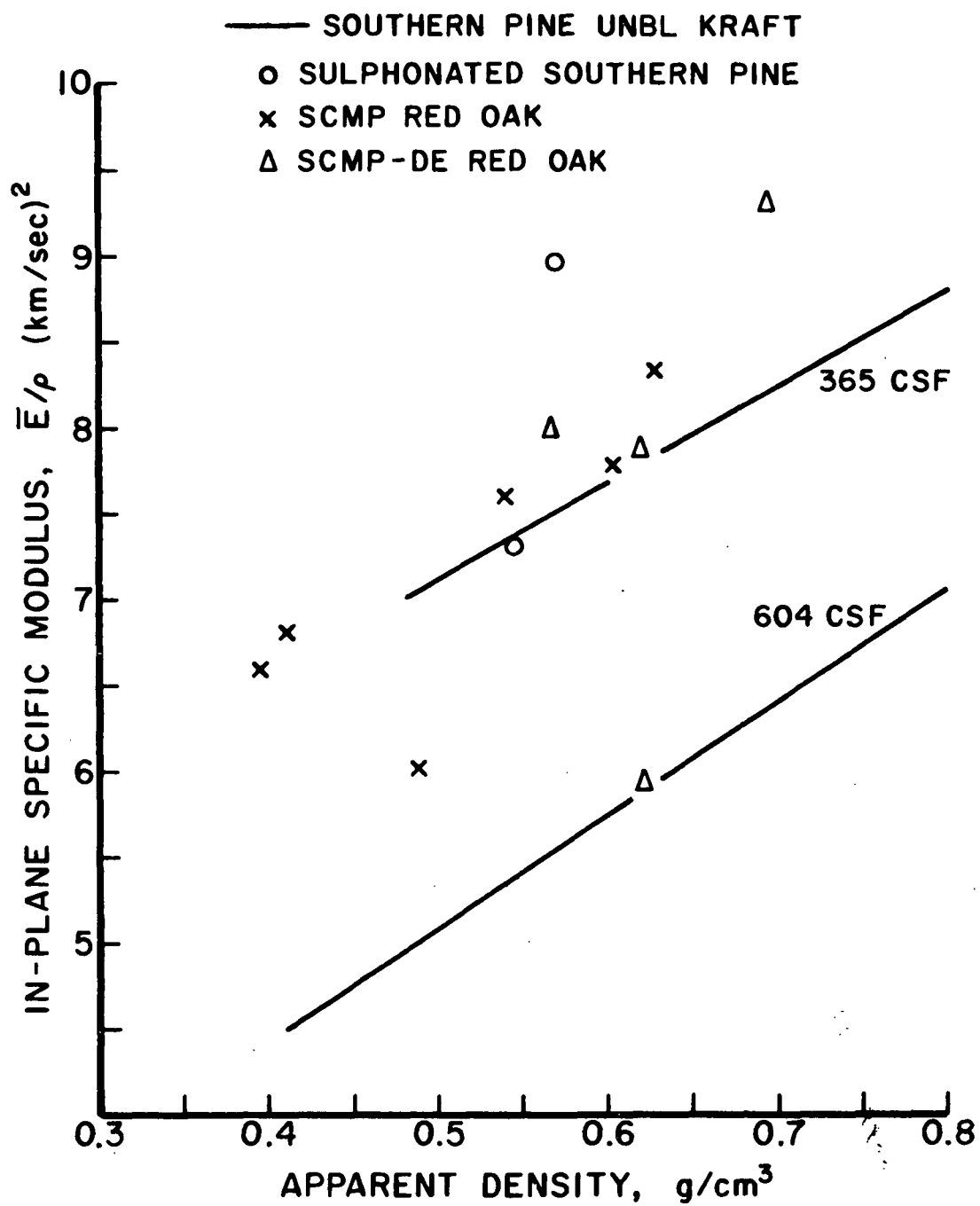
PROCESS VARIABLES

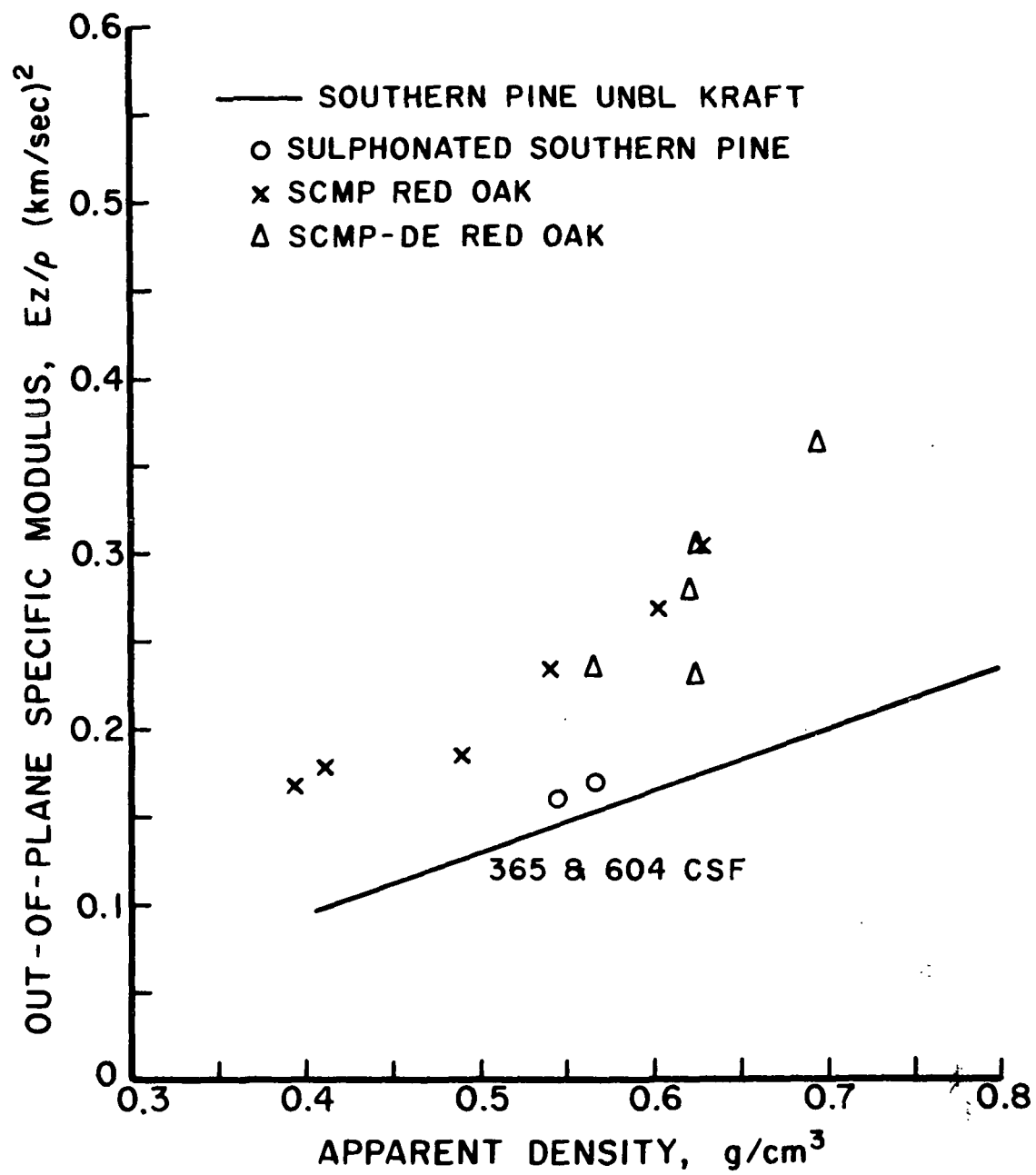
- WET PRESSING
- WET PRESS FELTS

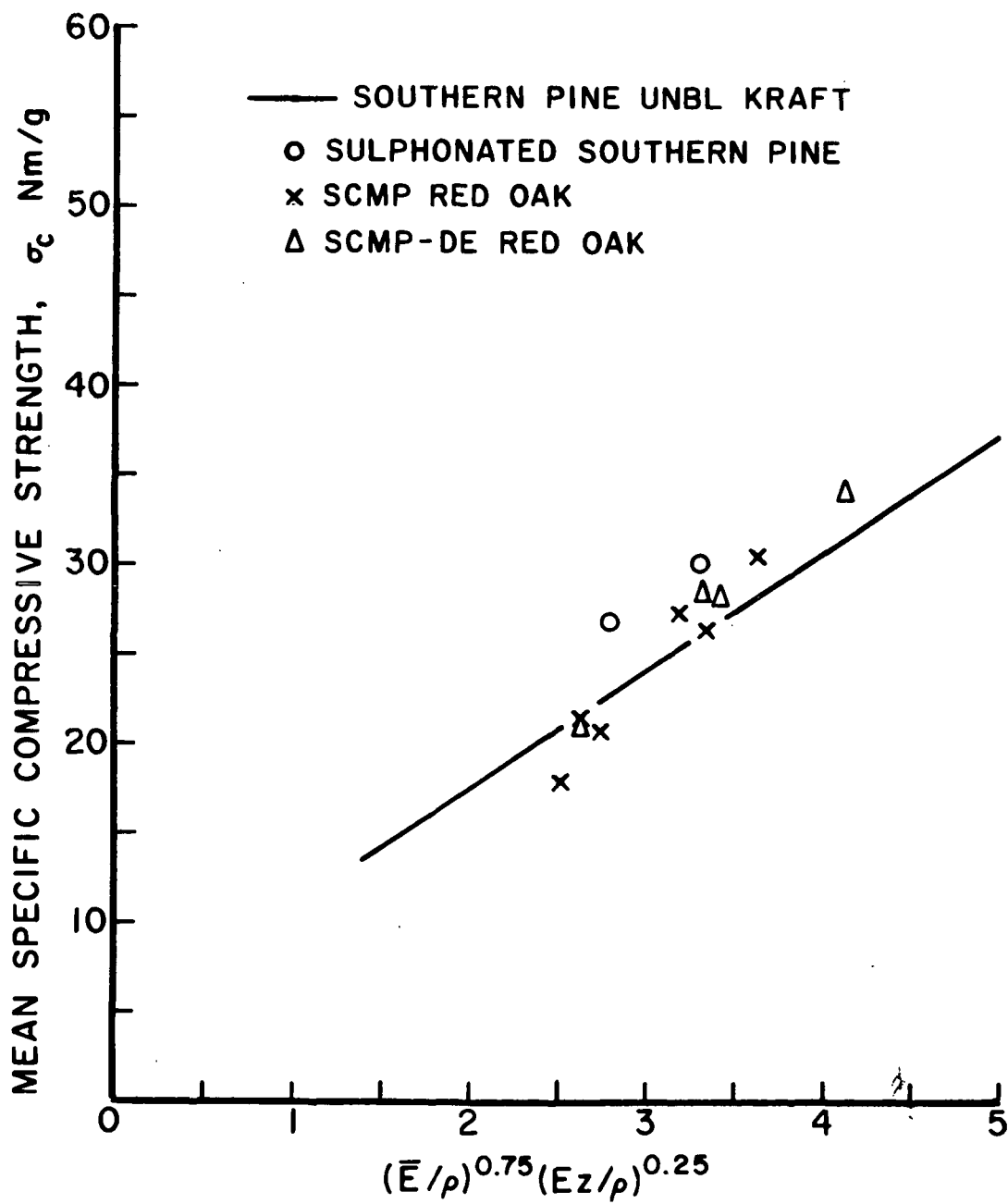


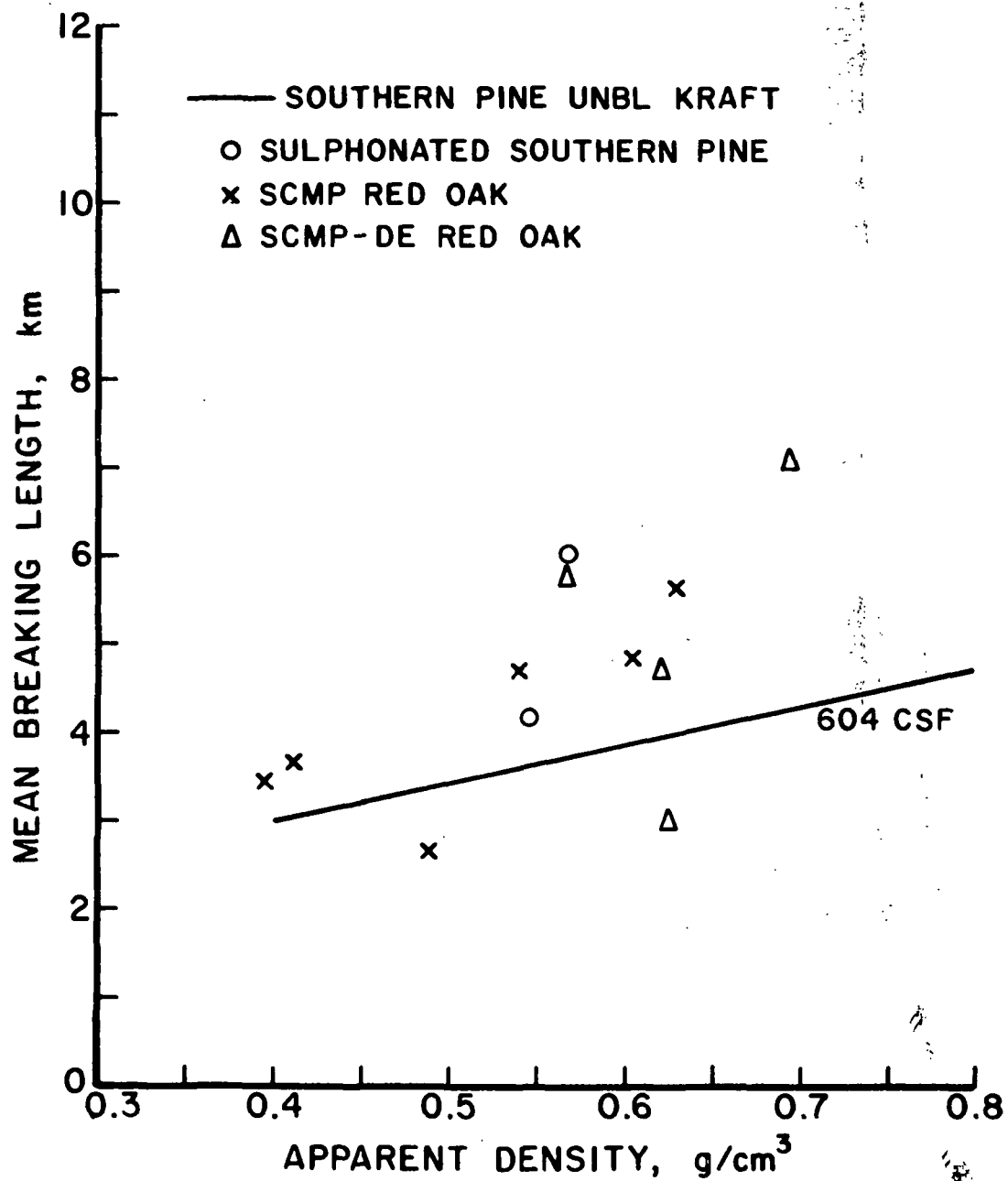
Compressive strength behavior of high yield pulps.









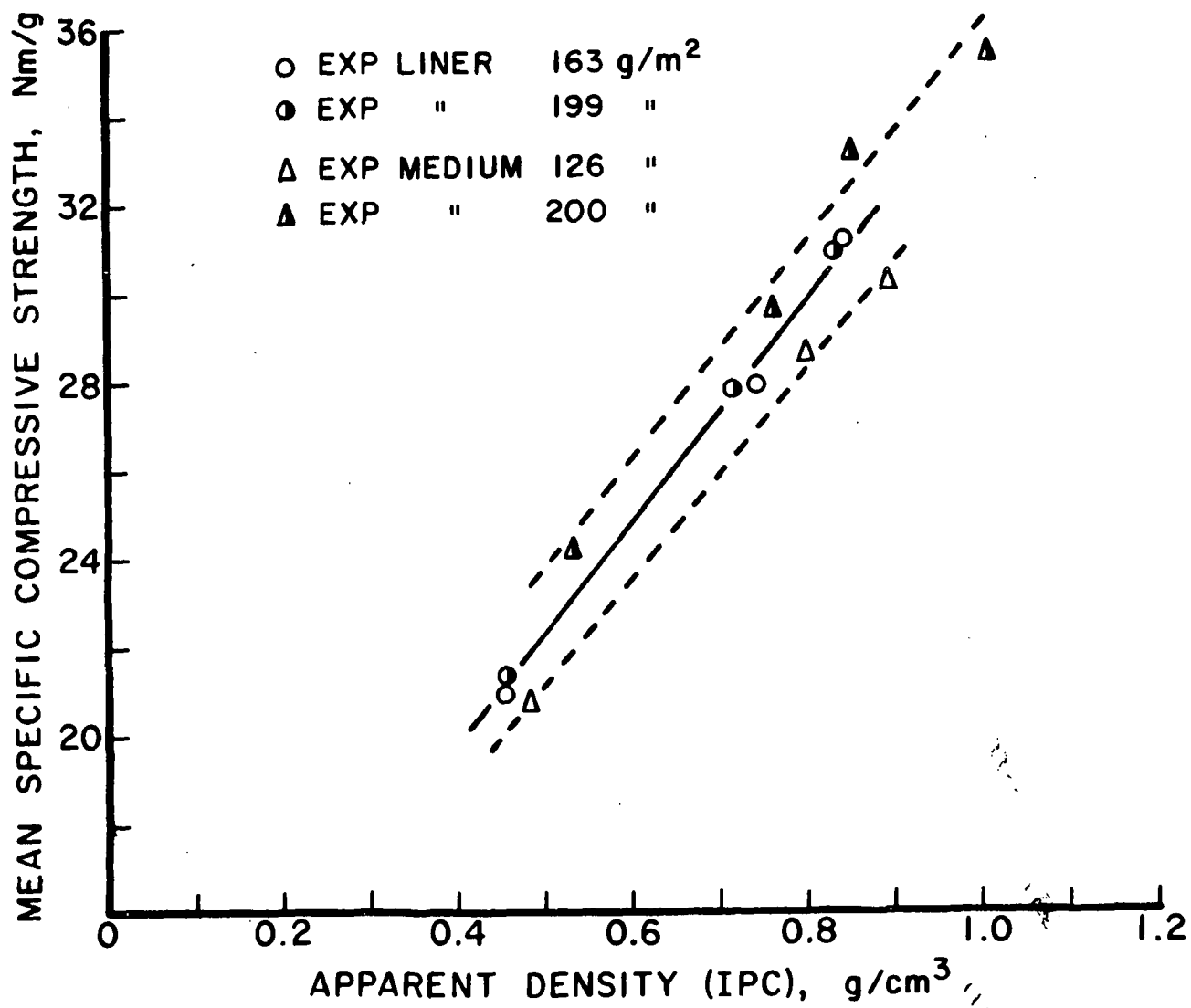


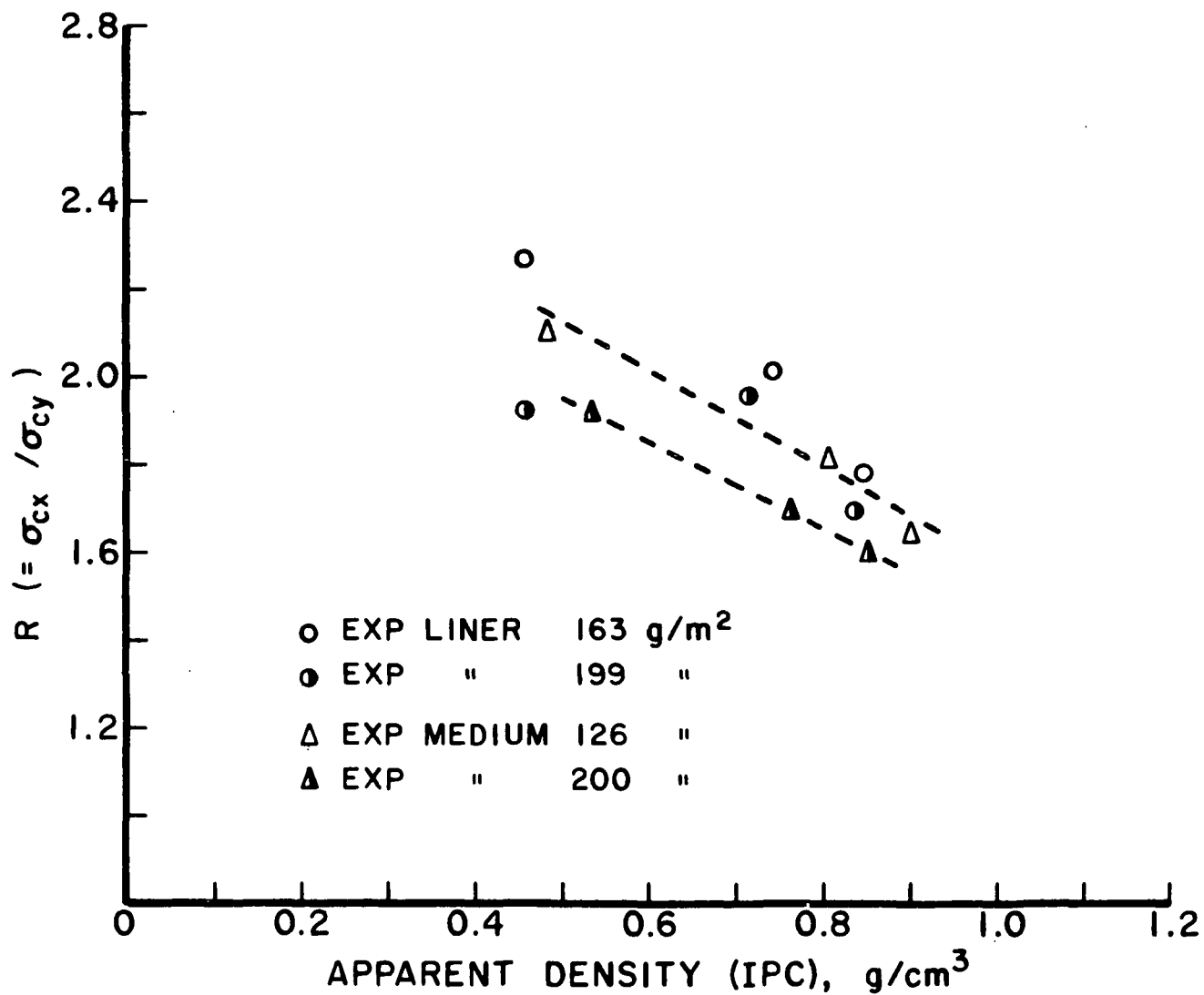
FUTURE WORK

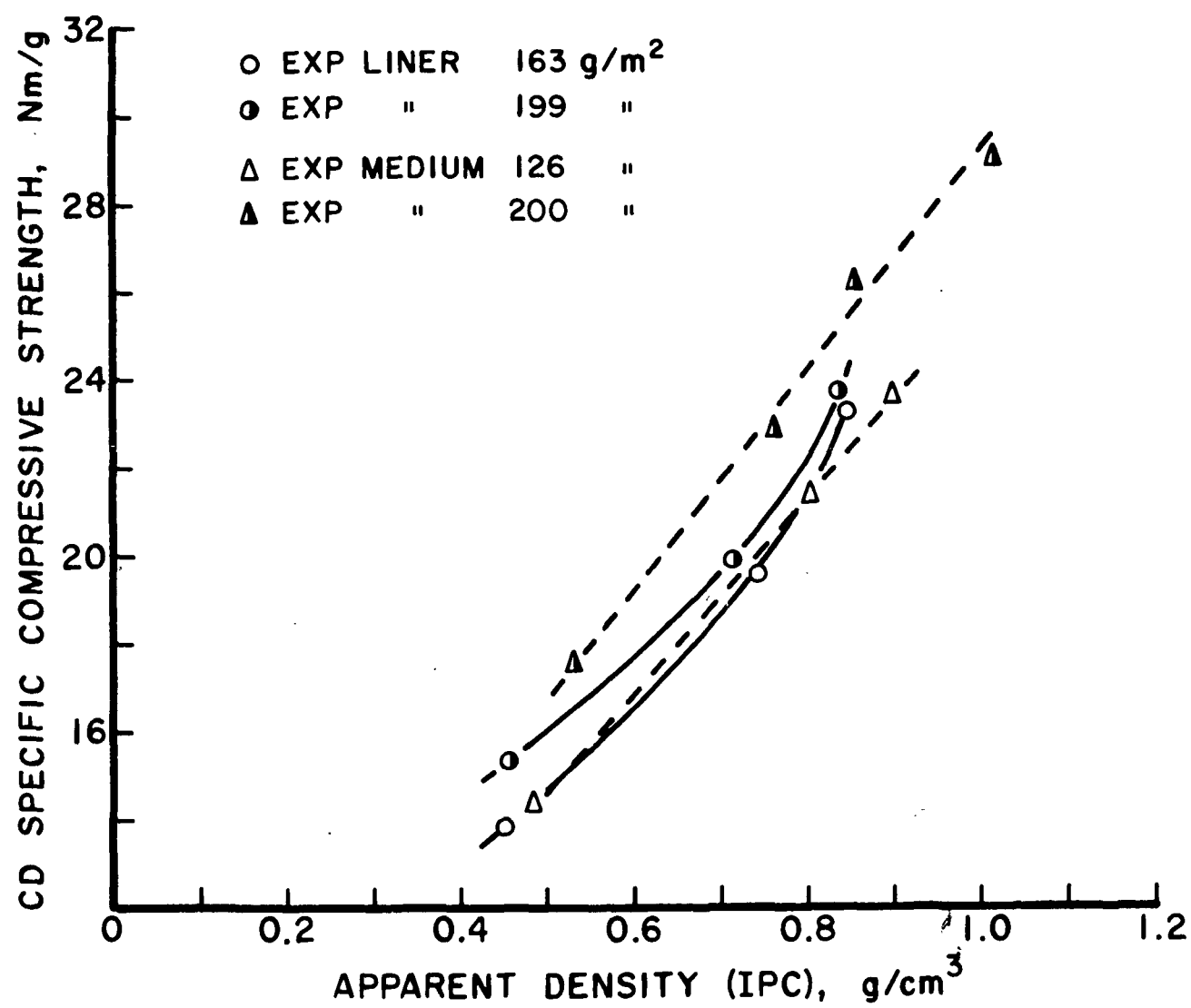
- HIGH YIELD PULPS
- POLYMER ADDITION

FUTURE WORK

- WET PRESSING
- WET PRESS FELTS







SECTION 8 .

PROJECT 3272

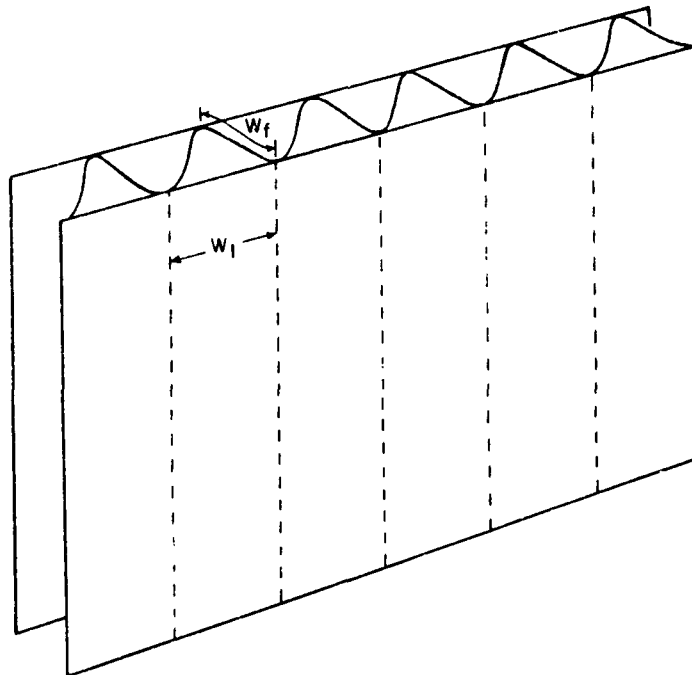
ANALYSIS OF BOARD STRUCTURES

ANALYSIS OF BOARD STRUCTURES

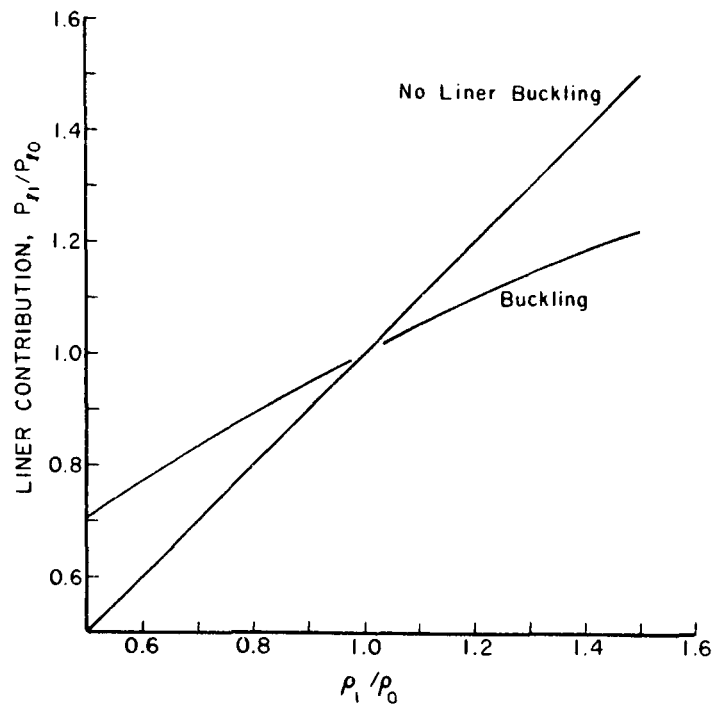
- PREDICT CONTAINER PERFORMANCE
- IDENTIFY CRITICAL PROPERTIES
- IMPROVE PERFORMANCE
 - PAPERMAKING
 - CONVERTING
 - DESIGN

COMBINED BOARD ECT MODELS

- COMPONENT COMPRESSIVE STRENGTH
- LOCAL BUCKLING
- ELASTIC STIFFNESS AND COMPRESSIVE STRENGTH



Corrugated board showing miniature liner and medium plate elements.



Estimated effects of density on the liner (or medium) contribution to combined board ECT strength (subscripts 1 or 0 denote the strength and density at a condition 1 relative to a reference condition 0).

INPUT DATA

- PARAMETERS FOR DESCRIBING STRESS-STRAIN CURVES
- COMPONENT THICKNESSES
- FLUTING GEOMETRY

OUTPUT

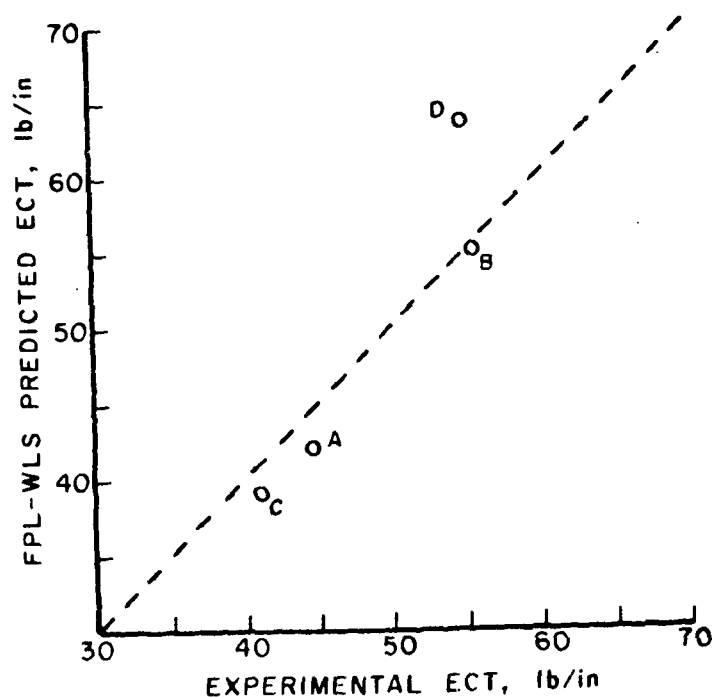
- ECT STRENGTH

FPL MODEL PREDICTS

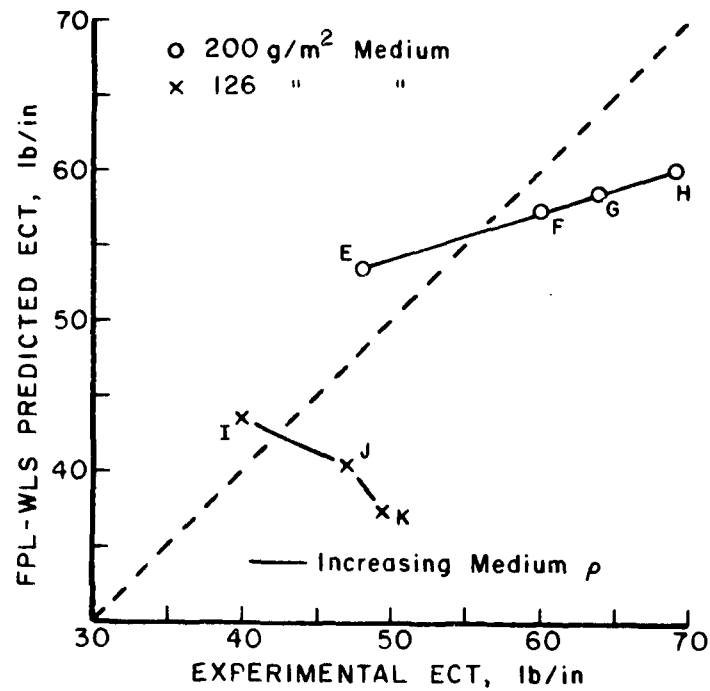
- MODE OF FAILURE INITIATION
- COMPONENT WHERE FAILURE INITIATED
- COMBINED BOARD ECT

EXPERIMENTAL DATA

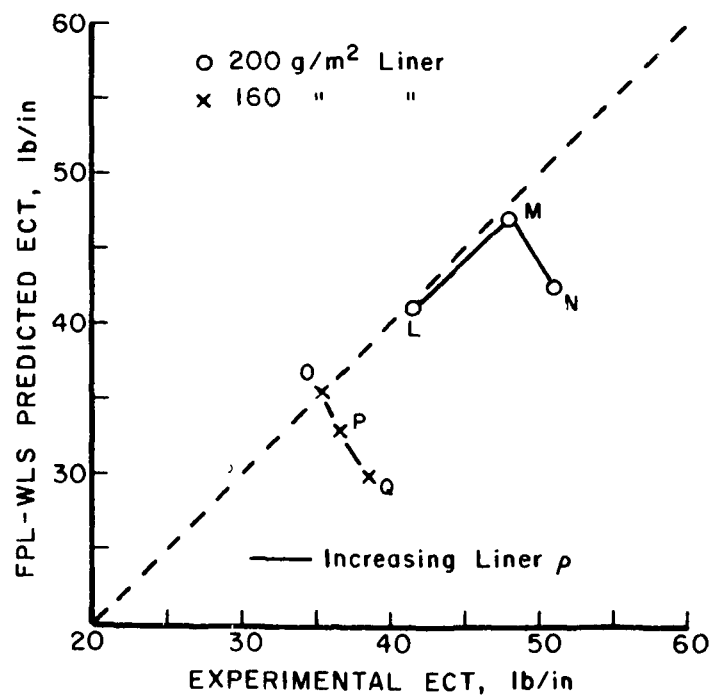
- 1) ORIENTATION STUDY
- 2) 200 g/m² DENSIFIED MEDIUMS
- 3) 126 g/m² DENSIFIED MEDIUMS
- 4) 200 g/m² DENSIFIED LINERS
- 5) 160 g/m² DENSIFIED LINERS



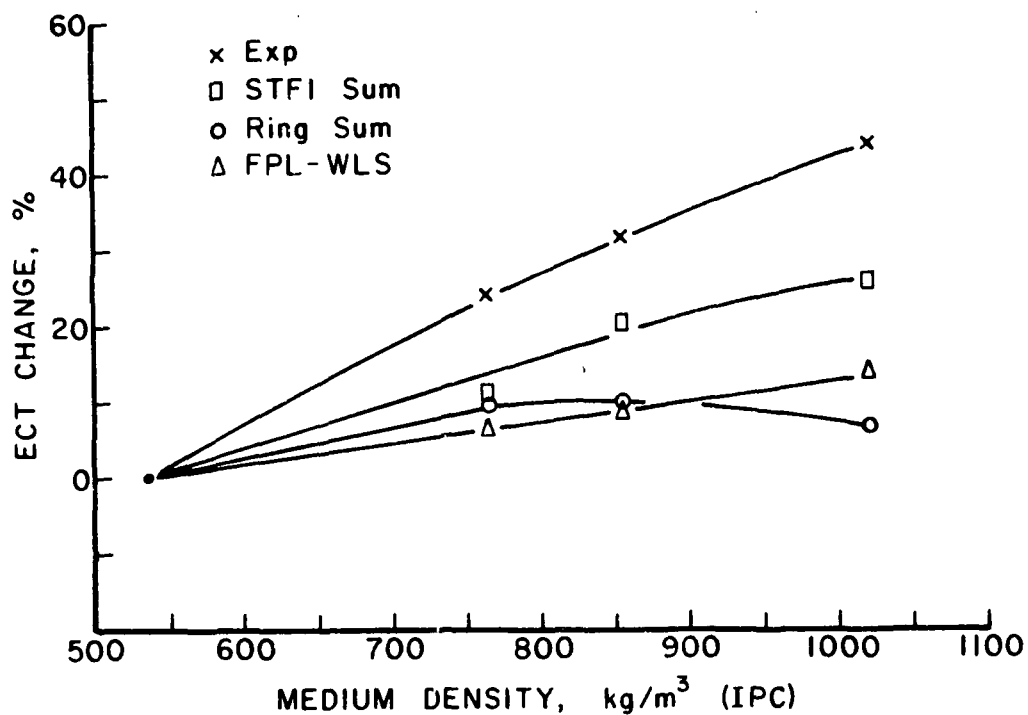
Effect of normal and reverse machine orientation. [(A) normal medium, (B) reversed medium orientation; (C) normal liners, (D) reversed liner orientations.]



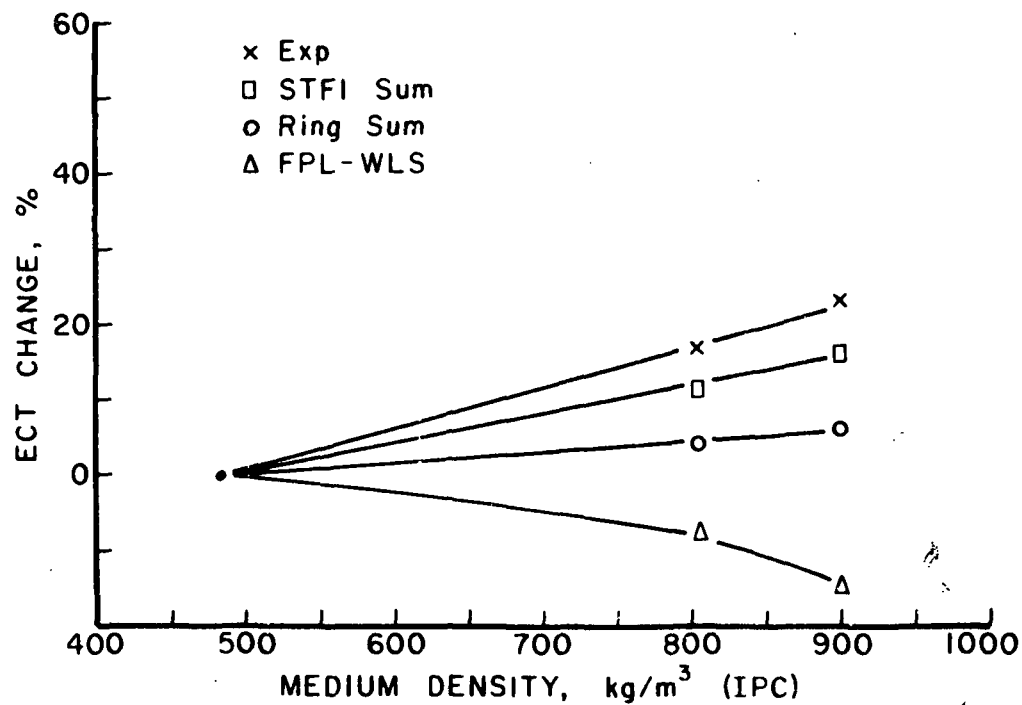
FPL-WLS predictions for boards made with medium of varying density.



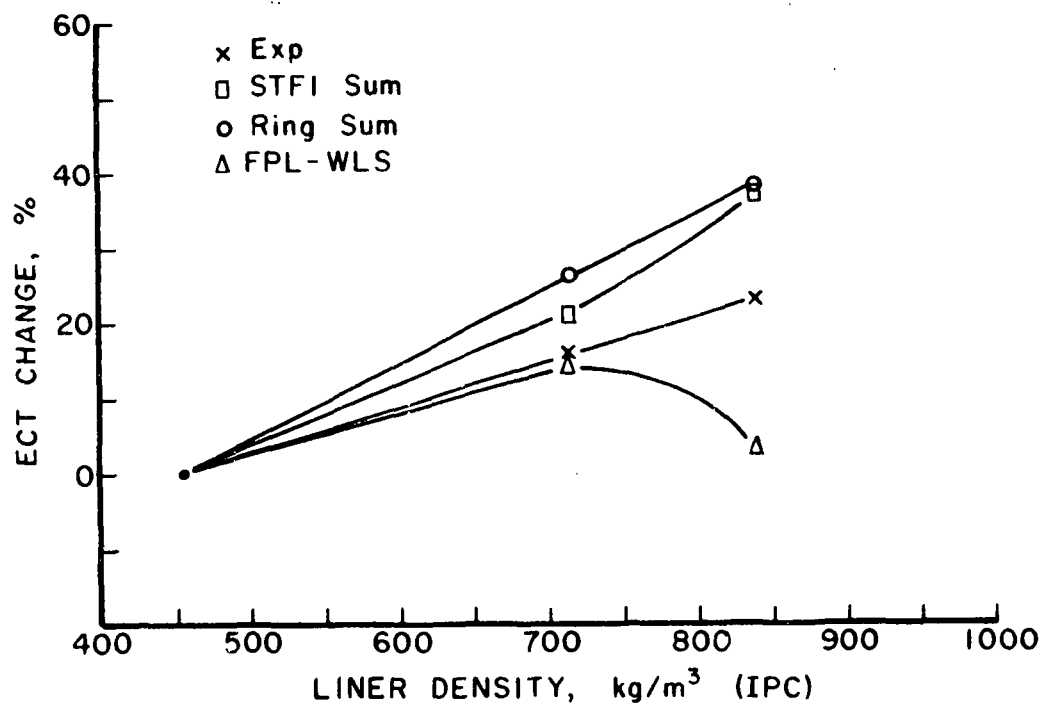
FPL-WLS predictions for boards made with liners of varying density.



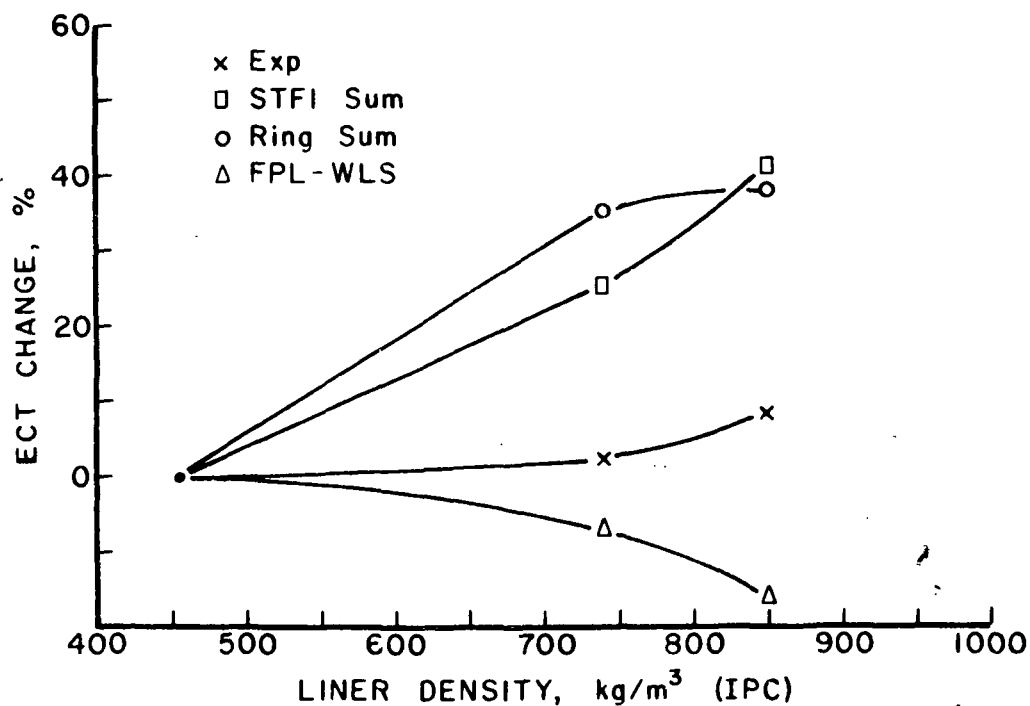
Comparison of % ECT changes for boards made with 200 g/m² mediums of varying density.



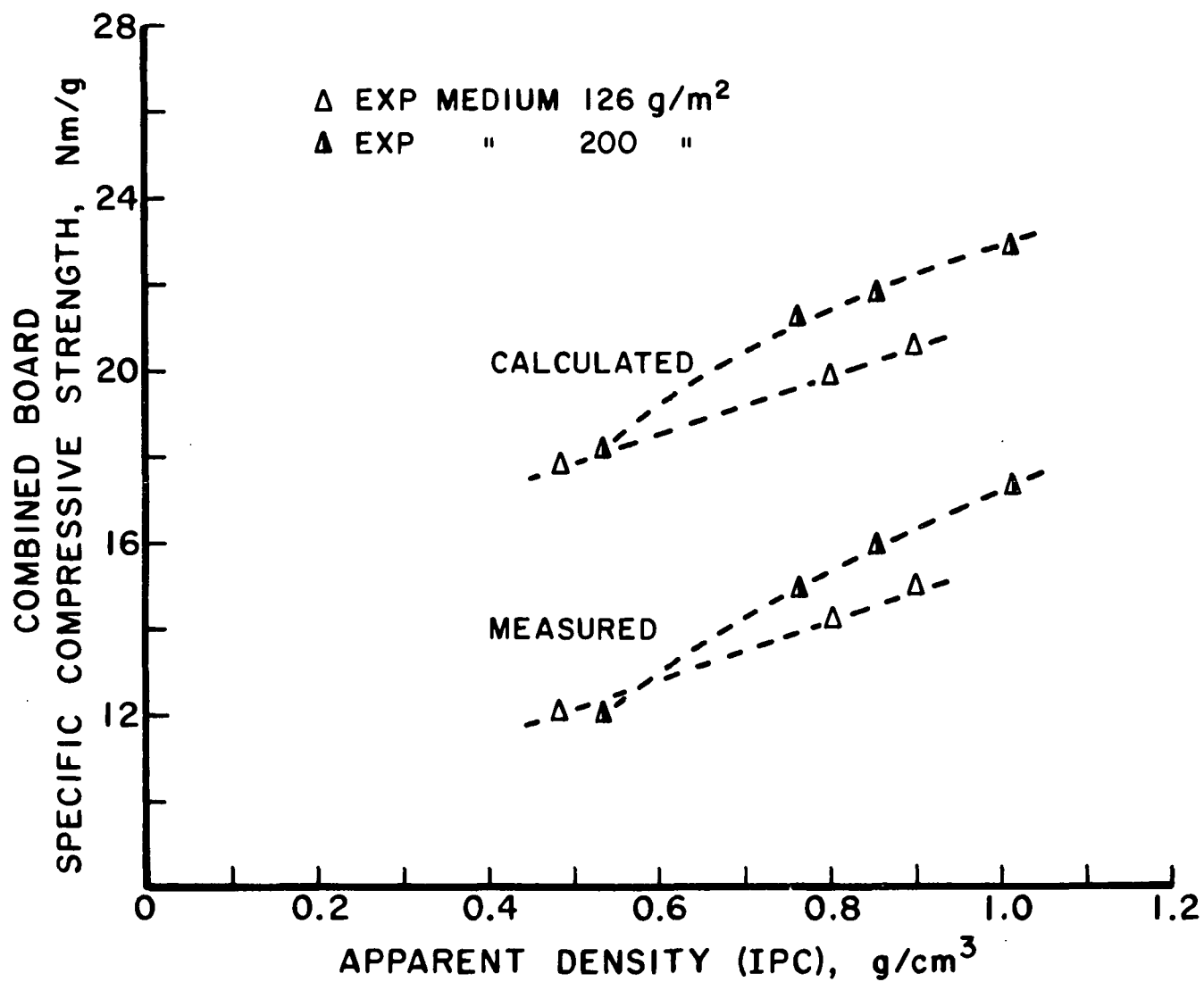
Comparison of % ECT changes for boards made with 126 g/m² mediums of varying density.

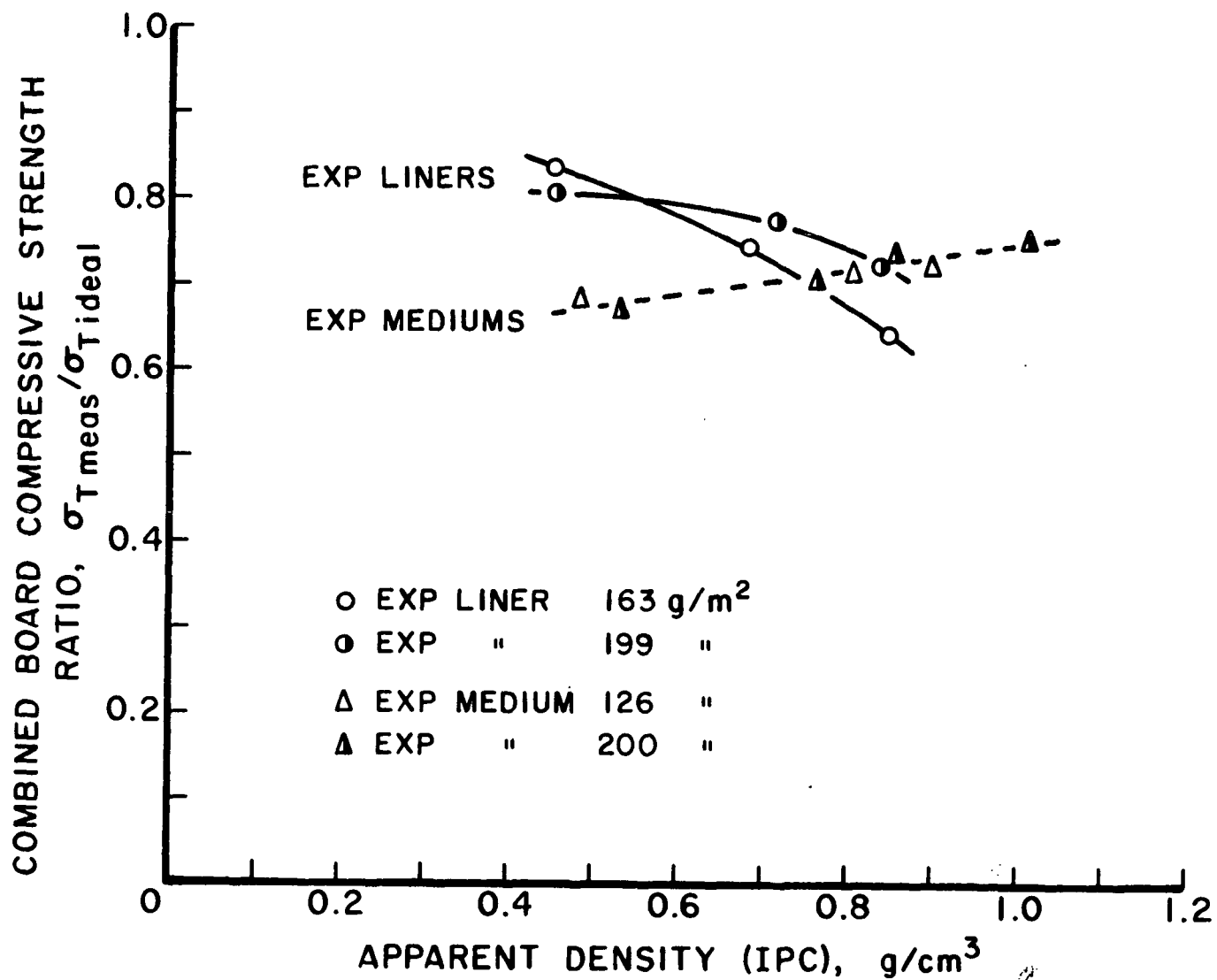


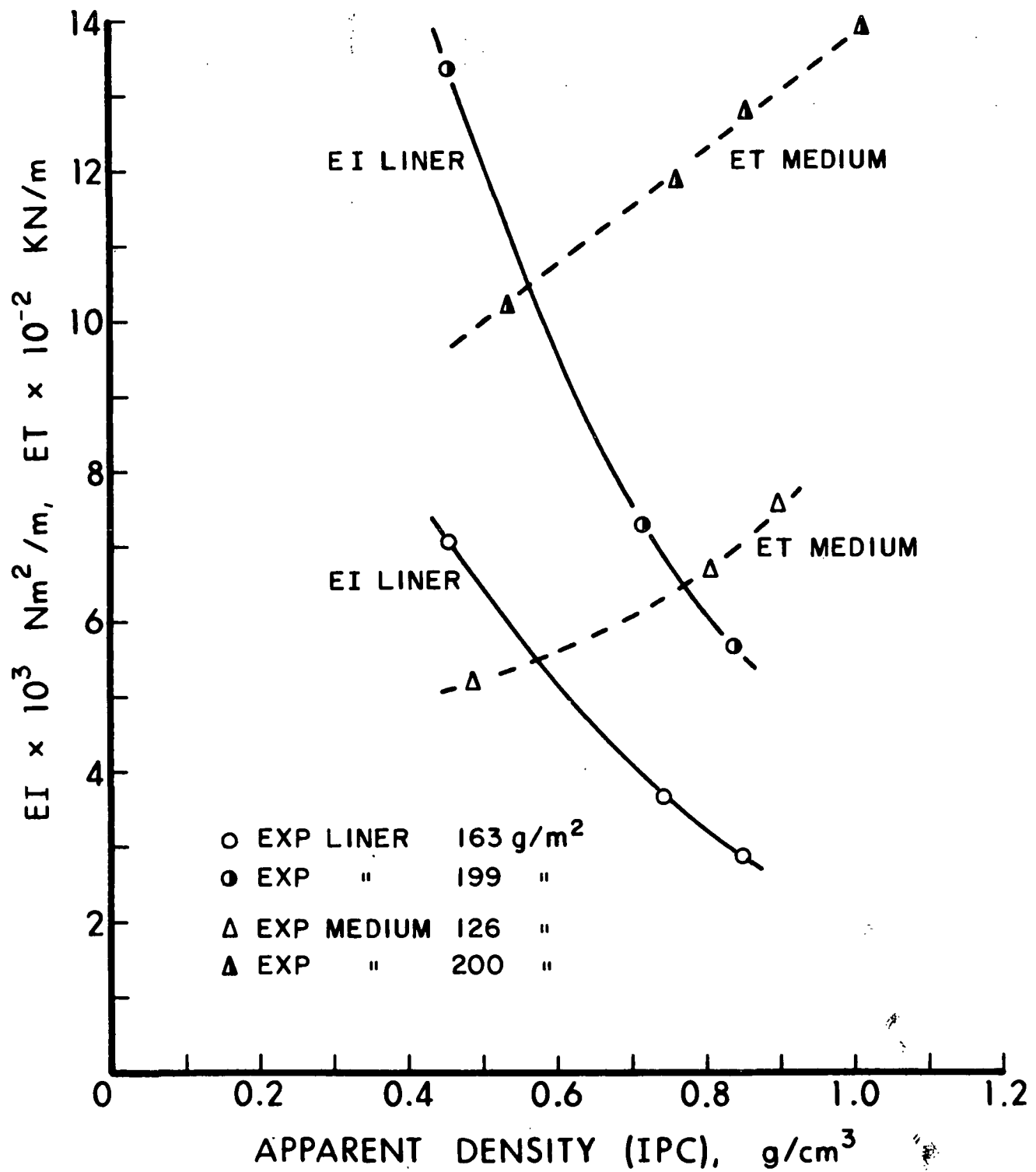
Comparison of % ECT changes for boards made with 200 g/m^2 liners of varying density.



Comparison of % ECT changes for board made with 160 g/m^2 liners of varying density.







SUMMARY OF EQUATIONS

$$P_T = 5.418 \text{ STFI}_L + 6.47 \text{ STFI}_M + 9.12$$

average error 5.0%, corr. coeff. = 0.96

$$P_T = 8.355 (\text{STFI}_L)^{0.85} (\bar{EI})^{0.15} + 6.163 \text{ STFI}_M + 4.616$$

average error 3.7%, corr. coeff. = 0.97

$$\sigma_T = 0.9 \alpha_L \sigma_L \left\{ \frac{\bar{EI}_L}{\bar{EI}_L + \bar{EI}_M} \right\}^{1.344} + \alpha_M \sigma_M$$

average error 1.9%